LNF-90/023

R.L. Golden, S.P.Ahlen, J.J. Beatty, H.J. Crawford, P.J. Lindstrom, J.F.Ormes, R.E. Streitmatter, C.R. Bower, R.M. Heinz, S. Mufson, T.G. Guzik, P.J. Wefel, S.A. Stephens, J.H. Adams, K.E. Krombel, A.J. Tylka, M. Simon, K.D. Mathis, P. Picozza, G. Barbiellini, G. Basini, F. Bongiorno, M. Ricci, A. Codino, C. De Marzo, B. Managelli, P. Galeotti, P. Spillantini, M. Bocciolini

WIZARD: A PROGRAM TO MEASURE COSMIC-RAY ANTIPROTONS AND POSITRONS, AND SEARCH FOR PRIMORDIAL ANTIMATTER

Estratto da: Nuovo Cimento 105 B, n.2, 191 (1990)

IL NUOVO CIMENTO VOL. 105 B, N. 2 Febbraio 1990

WiZard: a Program to Measure Cosmic-Ray Antiprotons and Positrons, and Search for Primordial Antimatter.

R. L. GOLDEN
Particle Astrophysics Laboratory, New Mexico State University - Las Cruces, NM

S. P. AHLEN and J. J. BEATTY
Department of Physics, Boston University - Boston, MA

H. J. CRAWFORD and P. J. LINDSTROM
Space Sciences Laboratory, University of California - Berkeley, CA

J. F. ORMES and R. E. STREITMATTER
NASA Goddard Space Flight Center - Greenbelt, MD

C. R. BOWER, R. M. HEINZ and S. MUFSON
Department of Physics, Indiana University - Bloomington, IN

T. G. GUZIK and J. P. WEFEL
Department of Physics and Astronomy, Louisiana State University - Baton Rouge, LA

S. A. STEPHENS
Tata Institute for Fundamental Research - Bombay, India

J. H. ADAMS, K. E. KROMBEL and A. J. TYLKA
Naval Research Laboratory - Washington, DC

M. SIMON and K. D. MATHIS
University of Siegen - Siegen, B.R.D.

P. PICOZZA
Dipartimento di Fisica, Università di Roma II «Tor Vergata» - Roma, Italia

G. BARBIELLINI
CERN - Geneve, Switzerland
Dipartimento di Fisica dell'Università - Trieste, Italia

G. BASINI, F. BONGIORNO and M. RICCI
Laboratori Nazionali INFN - Frascati (Roma), Italia

A. CODINO
Dipartimento di Fisica dell'Università - Perugia, Italia
INFN - Sezione di Perugia

C. DE MARZO and B. MANAGELLI
Dipartimento di Fisica dell'Università - Bari, Italia
INFN - Sezione di Bari

P. GALEOTTI
Laboratori di Cosmogeofisica del CNR - Torino, Italia

P. SPILLANTINI and M. BOCCIOLINI
Dipartimento di Fisica dell'Università - Firenze, Italia
INFN - Sezione di Firenze

(ricevuto l'8 Gennaio 1990)

Summary. — In this paper the WiZard experiment to be performed at the U.S. Space Station Freedom is presented. The apparatus will operate at the Astromag facility as a magnetic spectrometer dedicated to the search of primordial antimatter in the cosmic radiation. Several additional questions in the field of astrophysics and cosmology like solar flares, the galactic anisotropy, spectra of heavier nuclei (from carbon to iron), gamma-ray astronomy and others will also be investigated with such an apparatus and are discussed as well. The configuration of the apparatus, its integration and the description of each detector is covered in detail. Ground and flight operations are described together with discussion on data reduction and analysis. Finally, the mission planning and the onboard crew operations are also outlined.

PACS 98.80 – Cosmology.
PACS 95.55 – Astronomical instruments.
PACS 96.40 – Cosmic rays.

1. – Introduction.

1·1. *Objectives and significant aspects.* – The observational objectives of the WiZard instrument are to measure the spectra of antiprotons, positrons and

IL NUOVO CIMENTO VOL. 106 B, N. 3 Marzo 1991

ERRATA

WiZard: a Program to Measure Cosmic-Ray Antiprotons and Positrons, and Search for Primordial Antimatter.

R. L. GOLDEN
Particle Astrophysics Laboratory, New Mexico State University - Las Cruces, NM

S. P. AHLEN and J. J. BEATTY
Department of Physics, Boston University - Boston, MA

H. J. CRAWFORD and P. J. LINDSTROM
Space Sciences Laboratory, University of California - Berkeley, CA

J. F. ORMES and R. E. STREITMATTER
NASA Goddard Space Flight Center - Greenbelt, MD

C. R. BOWER, R. M. HEINZ and S. MUFSON
Department of Physics, Indiana University - Bloomington, IN

T. G. GUZIK and J. P. WEFEL
Department of Physics and Astronomy, Louisiana State University - Baton Rouge, LA

S. A. STHEPHENS
Tata Institute for Fundamental Research - Bombay, India

J. H. ADAMS, K. E. KROMBEL and A. J. TYLKA
Naval Research Laboratory - Washington, DC

M. SIMON and K. D. MATHIS
University of Siegen - Siegen, B.R.D.

P. PICOZZA
Dipartimento di Fisica, Università di Roma «Tor Vergata» - Roma, Italia

G. BARBIELLINI
CERN - Geneva, Switzerland
Dipartimento di Fisica dell'Università - Trieste, Italia

G. BASINI, F. BONGIORNO and M. RICCI
Laboratori Nazionali INFN - Frascati (Roma), Italia

A. CODINO
Dipartimento di Fisica dell'Università - Perugia, Italia
INFN - Sezione di Perugia

C. DE MARZO and B. MARANGELLI
Dipartimento di Fisica dell'Università - Bari, Italia
INFN - Sezione di Bari

P. GALEOTTI
Laboratori di Cosmogeofisica del CNR - Torino, Italia

P. SPILLANTINI and M. BOCCIOLINI
Dipartimento di Fisica dell'Università - Firenze, Italia
INFN - Sezione di Firenze

(*Nuovo Cimento B*, **105**, 191 (1990))

PACS 98.80 – Cosmology.
PACS 95.55 – Atronomical instruments.
PACS 96.40 – Cosmic rays.
PACS 99.10 – Errata.

The name of one of the authors has been unluckily misprint. We publish here above the correct version, B. MARANGELLI instead of B. MANAGELLI, sincerely apologizing to the author.

Direttore responsabile: RENATO ANGELO RICCI

Questo fascicolo è stato realizzato in fotocomposizione dalla Monograf, Bologna
e stampato dalla tipografia Compositori, Bologna
nel mese di marzo 1991

Questo periodico
è iscritto
all'Unione Stampa
Periodica Italiana

nuclei to high energies and to search for primordial antimatter. The WiZard geometry factor for measuring antiprotons and positrons is $0.1\,m^2\,sr$. For searches for primordial antimatter the geometry factor is $0.4\,m^2\,sr$. The WiZard instrument will be able to measure magnetic rigidities (momentum/charge) up to its maximum detectable rigidity of over 1 TeV/c. Data gathered with the WiZard instrument will relate to a wide range of fundamental issues. These include the i) role of Grand Unified Theories in Cosmology in relation to antimatter and dark matter, ii) understanding of the acceleration and propagation of cosmic rays, and iii) role of solar, terrestrial and heliospheric relationships to energetic particle propagation in the heliosphere. The WiZard observations and their implications will complement information gathered from the Great Space Observatories ground-based cosmic-ray experiments.

1'1.1. Objectives and their importance. In this section we first describe primary objectives, for which this experiment is designed and optimized, and summarize additional objectives obtainable from the same data. All these have great significance in a variety of fields and therefore the order in which they are listed under each category does not necessarily reflect their order of importance.

Primary objectives.

1) *Search for antimatter.* Detection of antimatter of primary origin in cosmic rays would be a discovery of fundamental significance. Cosmic-ray searches that have been made so far have yielded only upper limits of one part in 10^4 for heavy nuclei ($Z > 2$) and several parts in 10^5 for helium [1, 2]. Antiprotons and positrons are not good indicators for the existence of primordial antimatter. This is because they are produced by collisions of the cosmic rays with the interstellar medium. If there is primordial antimatter, antihelium is the most likely form to be detected in cosmic rays. This is because in cosmological predictions of the primordial composition of the universe and in stellar composition, helium is the next most abundant element to hydrogen. WiZard will be capable of detecting antihelium with a sensitivity of one part in 10^8. Similarly search for heavier antinuclei will be carried out with a sensitivity of a few parts in 10^7.

2) *Antiproton spectrum.* Antiprotons have been observed in the cosmic rays since 1979 [3, 4]. One feature of the observed flux is that, at high energies, it appears to be 3 times higher than that expected if the antiprotons are produced by interactions of the cosmic rays with the interstellar medium. The over-abundance of antiprotons has led to speculations of their origin ranging from models where the antiprotons are produced in shrouded supernovae [5], to annihilation of Majorana fermions created during the Big Bang [6]. Other models explain the excess in terms of how cosmic rays may propagate in the Galaxy (for

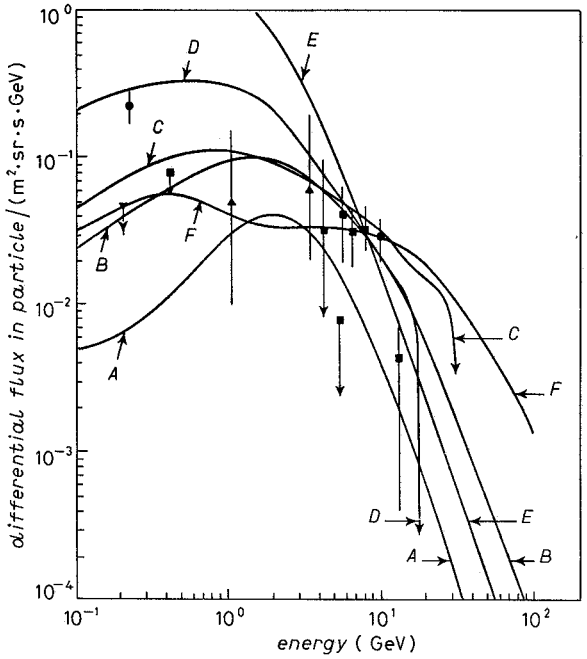

Fig. 1. – Antiproton energy spectra *A*: leaky box; *B*: closed galaxy; *C*: acceleration in dense cloud; *D*: dark matter annihilation; *E*: mini black holes; *F*: extra galactic.

a review see [7]). These speculations predict different energy spectra at high energies as shown in fig. 1 [8]. Because of atmospheric backgrounds and limited flight times balloon-borne experiments can only measure the energy spectrum of antiprotons up to about 20 GeV. In addition, the sensitivity of the balloon observations is limited by the difficulty in eliminating large flux of atmospheric secondary particles. WiZard will be able to measure the energy spectrum of antiprotons up to 300 GeV with a sufficient sensitivity to i) look for the signature of dark matter candidates, ii) establish contributions from different production mechanisms, iii) examine various propagation models and iv) identify the effect of Galactic modulation (if a portion of the antiprotons are of extragalactic origin).

3) *Electron and positrons.* Electrons and positrons are unique among cosmic rays because they are the lightest charged leptons. Because of their low mass, high-energy electrons and positrons undergo interactions with the interstellar medium which result in severe energy losses at high energies. While most of the observed e^- are believed to be of primary origin, the origin of e^+ is yet to be established. This is evident from the number of hypotheses for the e^+ spectra shown in fig. 2 [7]. The energy spectrum of e^- is measured up to about 1 TeV with large uncertainties [9-11] and the e^+ spectrum has been measured up to about 30 GeV [12-15] but the statistics and experimental agreement are poor.

The WiZard experiment will measure accurately the spectra of e^- and e^+ up to 1 TeV and 300 GeV, respectively. Their spectral shapes provide information on the i) acceleration of e^- and the distribution of acceleration sites on time scales of about 10^5 y, ii) cosmic-ray lifetime, and the physical conditions in the containment volume, iii) magnitude of re-acceleration with interstellar shock waves, and iv) origin and propagation of e^+ in relationship with antiprotons.

4) *Spectra of nuclei.* WiZard will measure energy spectra of nucleonic components up to carbon with unprecedented accuracy over 3 decades in energy. These precise measurements will answer many basic questions such as: i) Are the accelerated spectra a simple power law? ii) Is the acceleration the same for all elements? iii) How much matter is traversed in the galactic space and in the source? iv) Does every species have the same propagation history? and v) How much reacceleration cosmic rays encounter in the interstellar space? WiZard will also provide for the first time a very precise temporal variation of all species as a function of rigidity.

Additional objectives.

1) *Study of solar flares.* Energy spectra of flare particles will be measured for the first time at relativistic energies for protons and electrons >4 GeV and for helium >2 GeV/n during major solar flares. The shape and possible cut-off in their spectra would provide clues to the i) acceleration mechanism and ii) size, extent and physical conditions of the accelerating regions.

2) *Solar-terrestrial relationship.* Two kinds of anisotropies will be studied at relativistic energies as a function of rigidity and species. *a*) Particle anisotropies resulting from the i) rotation of the Sun, ii) diurnal and semidiurnal waves, and iii) Forbush decreases and recoveries; and *b*) North-South (N-S) anisotropy between $+28°$ latitudes to study its relationship to the i) intensity and duration of solar flares, ii) interplanetary magnetic field components, and iii) latitudinal angular distance of the neutral sheet from the Earth. Such information will be used to derive the rigidity dependence of the cosmic-ray radial gradient.

3) *Galactic anisotropy.* From the sidereal variations observed from this experiment, unidirectional and bidirectional anisotropies of cosmic rays in the local interstellar space will be derived as a function of rigidity [16]. Corrections for spurious anisotropy of solar origin will be made using N-S anisotropy measured by the same instrument [17]. The advantage of this experiment over the existing ones, using muon and neutron detectors, is the elimination of uncertainties arising from the atmospheric variations and the energy of the primary particle.

4) *Geomagnetic effect.* The suppression of rigidity cut-off resulting from the effect of solar flares, magnetic storms, etc. will be studied over a wide range

of latitude and longitude. Such information can be used to model the magnetic field perturbations in a realistic manner. Preliminary studies of the slow temporal variation of the geomagnetic field can be made using a similar technique.

5) *Spectra of heavier nuclei.* Measurements of the energy spectra of elements from carbon through iron can be made to energies of 500 GeV. Such measurements require a minor retuning of the instrument. Charge resolution will vary from 0.2 charge units at carbon to 0.3 charge units at iron.

6) *Gamma-ray astronomy.* WiZard will be in an «all sky survey mode» as a gamma-ray spectrometer. It has the potentiality of exploring the Universe from 1 GeV to 1 TeV with a resolution of 1% in energy (at the lower energies) and better than a few arc minutes in angle. However, its collecting power is about 1% of EGRET, which is to be launched as a part of the Gamma Ray Observatory, and only a few gamma-rays >10 GeV are expected from known sources. Therefore, WiZard will be in gamma-ray mode to i) examine its potentiality as a high-resolution gamma-ray spectrometer in the unexplored region >10 GeV, ii) determine the spectra of sources and diffuse background in a limited energy region and iii) search for and determine the spectrum of intense flare sources that might appear. It should also be noted that the WiZard calorimeter could be operated as a gamma-ray detector independent of the magnet spectrometer portions of WiZard. It has a 1 m^2 area, 100% detection efficiency, good energy resolution, and an angular resolution of better than 1 degree.

1·1.2. Relevance of these objectives to other fields.

1) *Cosmology.* Detection of antimatter in cosmic rays would provide direct evidence of the existence of antimatter in the universe [18]. It is believed that the matter/antimatter asymmetry in nature results from the symmetry breaking (violation of baryon number, C and CP) associated with the Grand Unified Theories (GUTs) [19] and the breaking of thermodynamical equilibrium soon after the Hot Big Bang [20]. The current upper limits for the antimatter content in cosmic rays are of the order of $3 \cdot 10^{-5}$. This level is only enough to tell that our galaxy does not contain stellar objects made of antimatter. The degree of asymmetry, if observed, will provide the basis for setting up realistic schemes under GUTs, which otherwise need to be tested by studying particle interactions at 10^{16} GeV. Remnants of interest from the Hot Big Bang are the Super Symmetry (SUSY) particles (Majorana fermions) as dark matter [21] and Mini Black Holes (MBH) [22]. SUSY particles would annihilate to antiprotons and e^+ in cosmic rays, and detection of their signature (*e.g.* [6]) in the energy spectrum of antiprotons (curve D in fig. 1) and e^+ (curve A in fig. 2) would be of fundamental importance to both cosmology and particle physics.

If MBH exist they would loose their mass by evaporation. During evaporation

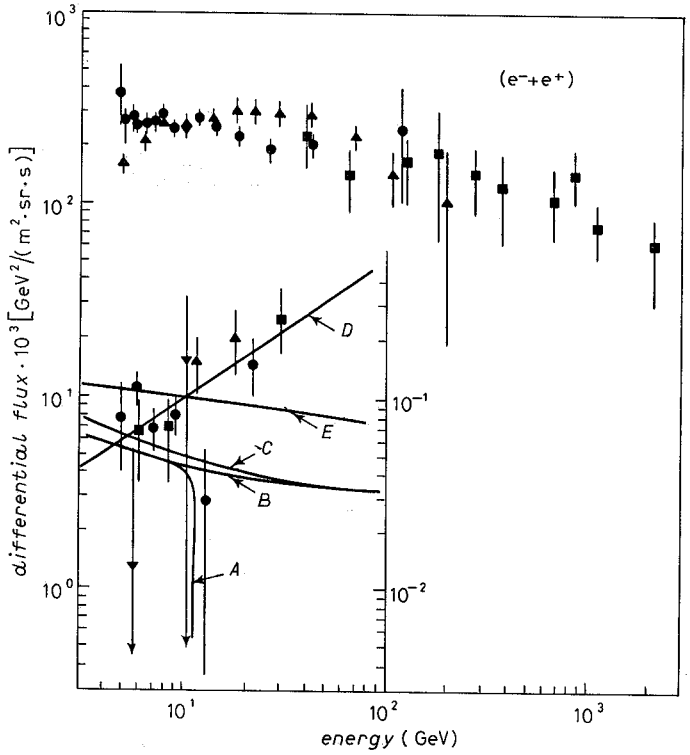

Fig. 2. – Positron energy spectra. *A*: dark matter; *B*: leaky box; *C*: closed galaxy; *D*: acceleration in dense clouds; *E*: pulsar.

of a MBH it is expected to radiate about 10^{30} erg (as quarks and gluons) during the last 0.1 s of its existence. As a result antiprotons are created and their identification in the antiproton spectrum (curve *E* in fig. 1) would provide credibility to the quantum gravity predictions.

2) *High-energy astrophysics.* Cosmic rays are associated with violent events occurring in nature and the information gathered from cosmic-ray studies is a key to the understanding of these phenomena (NRC Astronomy Committee Survey Report, 1982). Knowledge of cosmic-ray phenomena has been helpful in modelling high-energy processes in the galaxy. For example, [23] have shown that the interaction of ultrahigh-energy cosmic rays from a compact object with its companion can inject a large amount of energy into its interior and consequently alter its course of evolution.

The pressure exerted by cosmic rays in the interstellar space is comparable with thermal, radiation and magnetic field pressure and thus cosmic rays play an important role in the galactic dynamics [24]. At the level of statistics expected from WiZard, deviations from power law energy spectra can be expected. The

measurement of these deviations will be of great help in understanding the possible acceleration mechanisms [25].

3) *Astronomy.* Cosmic-ray nuclei interact with matter and produce gamma-rays through high-energy collisions. Electrons interact with magnetic and radiation fields through synchrotron and inverse Compton processes. Electrons also interact with matter by emitting bremstrahlung radiation. The bremstrahlung radiation is in the radio to gamma-ray wavelength regime. As a result of these interactions, cosmic rays play an important role in a wide range of astronomical observations from radio waves to ultrahigh-energy gamma-rays. Thus, WiZard will complement observations from the Great Space Observatories.

4) *Other areas.* This investigation will give for the first time a wealth of information (as a function of rigidity and species) on anisotropies and secular variations at relativistic energies. This data will provide the basis for understanding high-energy processes in the Solar System, which require interdisciplinary cross-fertilization of fields, such as solar physics, heliospheric physics, magnetospheric physics and solar-terrestrial physics.

1·1.3. Relationship to other cosmic-ray work. Observations of primary cosmic rays have been carried out using balloon and space-borne instruments over the last few decades. Although these measurements were often limited in energy range and collecting power they have provided the foundation for many current ideas and raised further questions relating to the understanding of cosmic rays. In this section we review current and past work in cosmic-ray physics which is relevant to this proposal.

Systematic study of the differential energy spectra of cosmic-ray nuclei at relativistic energies was carried out in the 1970's when magnetic spectrometers, deep calorimeters and efficient Čerenkov detectors were developed for balloon-borne experiments [26-29]. These developments yielded immediate results showing that secondary nuclei in cosmic rays have steep spectra compared to the primary cosmic rays. This is interpreted as a decrease in the amount of interstellar matter traversed by cosmic rays at higher energies. Many theoretical models were put forward to explain this observation (see eg. [30-32]). The HEAO-C3 satellite experiment provided additional detailed information on the energy spectra up to about 50 GeV/n and further indicated that the spectra above 10 GeV/n may not be a smooth power law [33]. Recent experiments carried out in Spacelab extended this study to even higher energies with very low statistics [34].

In the case of the electron component, balloon-borne experiments using different tecniques were deployed during the 1960's to measure the spectrum up to a TeV [35]. The uncertainty in these investigations was so large that the flux values varied over one decade in any energy band [36]. In spite of this, the

importance of this spectrum in relation to universal black-body radiation and astronomy in general was realized. A few experiments were later undertaken using improved techniques [9-11] but the results, although consistent, are still hampered by low statistics.

Attempts to measure antiprotons and e^+ using balloon-borne experiments were made from early 1960's, but only meager data are available to date [10, 12-15, 37-39]. Theoretical speculations relating to these components are sensitive to many fundamental ideas in astronomy and cosmology. These speculations have provided a strong motivation for performing these difficult experiments [7]. In all these investigations no single experiment could cover the energy spectrum over a range of 2 decades.

Balloon-borne experiments during the next 5 years could improve the situation only over a limited energy region. We can expect that e^- and e^+ measurements will be restricted to about 200 and 40 GeV, respectively, due to limited exposure factors and atmospheric backgrounds. The antiproton spectrum will probably be measured only up to 20 GeV due limited flight times and the vast background of atmospheric moons.

In general, experiments measuring secondary cosmic rays from balloons suffer a basic limitation at energies above $(20 \div 50)$ GeV. This limitation is because the interstellar matter traversed by cosmic rays is less than $2\,g/cm^2$ above 50 GeV/n. Therefore, above a few tens of GeV/n, the amount of atmosphere above a balloon payload (typically $5\,g/cm^2$) produces more secondaries than those produced in the galaxy.

It is clear from the above discussion that the objectives described in this proposal cannot be achieved during the next decade using balloon-borne experiments. The limitations to ballooning arise from the effects of the overlying atmosphere and limited statistics. WiZard will surpass all available measurements in accuracy and in energy range. In the case of particles such as positrons and antiprotons, spectra will be determined over 2 decades in energy to test many predictions. Limits on antimatter/matter asymmetry will be set very close to the level of *CP* violation. Spectra of primary components of cosmic rays will be measured over 3 decades in energy with sufficient accuracy to look for structures in the spectrum. The availability of long duration exposure provides the first opportunity for a detailed study of temporal variations of cosmic rays at relativistic energies.

1·2. *Investigation approach.*

1·2.1. Concept. The WiZard experiment utilizes an array of particle detectors mounted on one end of the Astromag magnet system. Figure 3 illustrates the detectors proposed for the WiZard experiment. In this paragraph we describe the basic concepts in the WiZard design. In later paragraphs we discuss the details of each detectors design and the overall performance of the instrument.

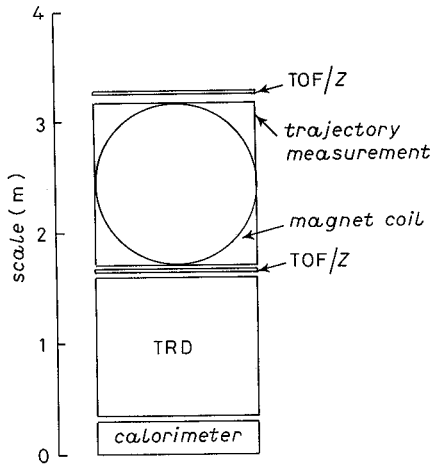

Fig. 3. – WiZard detector configuration.

Starting from the top, the instrument includes a pair of time-of-flight (TOF) detectors, a tracking system and another pair of TOF detectors. The tracking system is an instrumented volume which allows an almost continuous measurement of a particles trajectory as the particle traverses the magnetic field produced by the Astromag coil. The TOF detectors measure the time required for a particle to traverse from the top plane to the bottom. Both the TOF and tracking system make measurements of the particles charge as it traverses the system. Taken as a unit, the TOF and tracking systems are all that is required for the search for primordial antimatter. The TOF tells the direction of flight of the particle and the magnitude charge. The tracking system allows determination of the particles rigidity and sign of charge. Great care has been taken in the design of this system to minimize the mass that must be traversed by particles being measured. Any extra mass introduced here results in increased chances of the particle undergoing interactions which increase the difficulty of interpreting the event.

To measure positron and antiproton fluxes, additional detectors are required. For example, an electron and an antiproton would be indistinguishable using the TOF and tracking systems described above. The transition radiation detector (TRD) and the calorimeter provide means for separately identifying light particles (*e.g.* electrons and positrons) from heavier particles (protons and antiprotons).

The total instrument TOF, tracking system, TRD and calorimeter constitute an array of particle detectors capable of identifying electrons, positrons, antiprotons, nuclei, and antinuclei over a wide range of energies. We have chosen types of detectors that allow cross-checks in observational technique. We have designed each detector so that it contains internal redundancy (for purposes of reliability and resolution).

The detectors are held together by a backbone structure which also serves as the shuttle launch carrier. The backbone structure includes the main on-board computer, low voltage supplies and a wiring harness. The individual detectors are mounted within a segmented pressurized container which is part of the backbone. Each of the pressure container segments houses a detector element. When WiZard is assembled the individual detector modules form a single pressurized volume with a low-mass entrance window for the cosmic rays. Each detector module incorporates its own computer/controller which is responsible for gathering the detector data passing the information to the central experiment computer. This approach is used to speed up the event processing and reduce the amount of information to be transferred. Table I summarizes the weights and power consumption levels for the WiZard instrument:

TABLE I. – WiZard *instrument weight/power breakdown.*

Element	Weight	Power
TOF	173	200
tracking system	525	150
TRD	325	200
calorimeter	1020	200
WiZard structure	500	0
WiZard central electronics	50	200
Total	2593 kg	950 watts

1·2.2. Methods/procedures. In this paragraph we describe how data is gathered by the WiZard experiment.

The traversal of a particle is recognized by an appropriately timed coincidence between the upper and lower TOF detectors. The WiZard experiment computer then checks the TOF data to see if the particle had a charge of 2 or more. It also checks to see if a usable track was found by the tracking system. If these criteria are met, the event is accepted for transmission to the ground. If the particle had a charge of 1, it is further required to 1) have usable track information and 2) penetrate the TRD and calorimeter systems. These additional requirements assure that enough information has been gathered to allow separate identification of antiprotons, protons, positrons, and electrons. The total geometric factor for charge = 1 triggers is $0.1\,m^2\,sr$. From charge 2 or more the geometric factor is $0.4\,m^2\,sr$.

1·3. *The* WiZard *team.* – The proposal team is a blend of experienced operators of balloon-borne cosmic-ray experiments and team members with extensive experience in ground-based particle accelerator observations. The team originally formed as a result of the team members participation in the

Astromag Facility Definition Study. As a result we have a long history of working together, both for Astromag, and in a number of collaborative research efforts (including balloon flights).

The basic concept for the instrument instrument comes from the designs of two balloon payloads incorporating superconducting magnet spectrometers. One is the NASA/NMSU balloon-borne magnet facility (BBMF) [40]. The other is the PBAR balloon payload built by a collaboration headed by Boston University [38]. The NASA/NMSU BBMF contains a magnet which is basically a 1/2 scale Astromag magnet. The BBMF magnet spectrometer has been in operation for 15 years. It was used for the initial discovery of antiprotons in the cosmic rays in 1979 [3]. The PBAR instrument was first flown in 1987 and is now being used for antiproton and isotopic composition experiments [41]. We draw heavily on the operational and observational experiences gathered with these two instruments. We have also incorporated in the design the very latest technological advances in elementary-particle measurements.

2. – Instrumentation.

2·1. *Instrument description.* – In this section we present detailed descriptions of the individual detector modules and the structure that ties them together. The instrument is made up of a modular pressurized volume, mounted in a structure which also acts as the launch carrier. The detector stack is 3.4 m tall and 1.5 m by 0.75 m in area. The cross-sectional shape was chosen to optimize the tracking system performance. The cosmic rays enter the experiment through

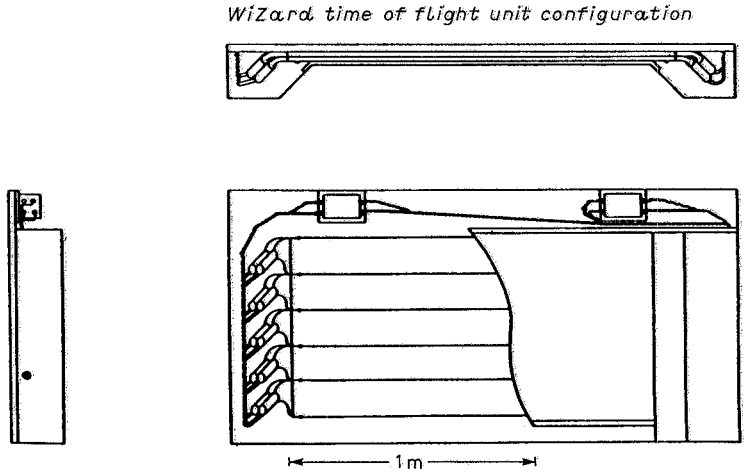

Fig. 4. – TOF detector configuration.

a thin window (less than $0.3\,g/cm^2$). We begin with the detectors (from top to bottom):

a) Time-of-flight. The time-of--flight (TOF) system serves as the basic trigger for WiZard. It also determines the direction of the cosmic rays and measures their charge. The TOF consists of 4 planes of 1 cm thick Bicron 404 Scintillator strips of size $(15 \times 160)\,cm^2$ (fig. 4). Each strip is viewed by a Hamamatsu R24090 photomultipliers. Passage of a particle through the 4 planes is noted by a high-speed logic array (fig. 5). A fast trigger signal is generated if

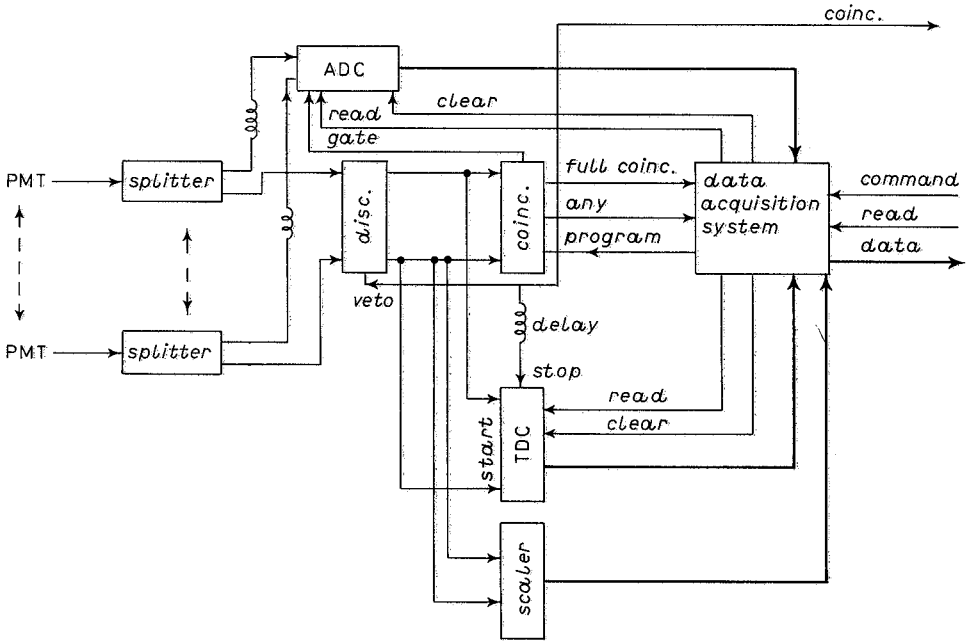

Fig. 5. – TOF electronics.

the particle's traversal time is within programmable limits. The trigger acts as a gate pulse which activates data aquisition in the other detector modules. The TOF processor system reads the time and pulse height information, eliminates information from phototubes not hit, and applies any other criteria (consistency, single track, etc.) which it may be programmed to perform. The resulting TOF message is then transferred, on request, to the central computer.

Performance requirements of the TOF are driven by the antimatter search. They are:

1) The TOF must unambiguously tell upward-going from downward-going particles (error rate $\ll 10^{-8}$).

2) The TOF must measure the magnitude of an incident particle's charge accurately enough not to misidentify a proton as helium. WiZard will measure a finite flux of antiprotons and the requirement that this will not contribute to any antihelium candidate sets an error rate of $2 \cdot 10^{-8}$ or better.

3) The TOF must provide sufficient position information to allow consistency checks with tracking information, and to facilitate multiple-particle events.

In normal operating mode, the TOF system has a dynamic range accommodating hydrogen to oxygen. In addition, the system has a low-gain operating mode in which the element spectra from oxygen to iron can be measured. The fourfold WiZard system will achieve a charge resolution of 0.2 or better through oxygen, a resolution of 0.3 or better for iron, and separation of charge one and two at better than 10^{-7}.

TOF measurement is an established technique and a time resolution of 50 picoseconds (ps) has been achieved [42]. A time resolution of 500 ps gives more than 20 standard deviations for the time difference between upward-going and downward-going particles in WiZard. Thus the time resolution required of the TOF is not stringent, even if one takes into account the non-Gaussian effect observed at large standard deviations [43].

The Hamamatsu R2490 phototube can be operated in high magnetic field with its axis parallel to the magnetic field [44]. A combination of these tubes and Bicron scintillators was used in a TOF system designed at GFSC [43] and flown in the NASA/BBMF [39]. That system is of the same approximate size and an operational resolution of 450 ps was achieved for relativistic particles. A fiberoptic system will be used to stimulate in-flight calibration of timing.

The time-of-flight detector assembly is designed to be a self-contained structural unit (see fig. 4). Its main structural element is a single piece of aluminum honey-comb panel, which also supports the light pipes, phototubes and electronics. The mechanical attachment of the TOF to the remainder of the detector assembly will be at each of the four corners of the TOF. The overall weight of the 4 TOF planes and their electronics is estimated to be 200 kg. The power consumed will be less than 200 watts.

There are 32 planes arranged as 6 at the top, 4 planes spread out, 12 planes in the middle, 4 more spread out, and 6 at the bottom.

b) Tracking detector. Several members of the collaboration have extensive experience in tracking systems, based on both multiwire proportional counters (MWPC) and drift chamber technologies. Our collaboration has three currently funded tracking system development programs underway. We find that for the WiZard experiment, the MWPC systems offer prompt read-out at an acceptable resolution (prompt readout allows use of track-quality tests in the trigger). Drift chamber systems offer better spatial resolution and a lower parts-count per

detector. One of the key activities of the phase 1 program is to do a comprehensive review of both MWPC and drift chamber systems. The final design may well be a hybrid MWPC-drift chamber system to take advantage of the strengths of these two approaches. The tracking system design presented here is mainly based on the system used for the NMSU balloon payload. This is principally because it is the system best understood at NMSU (it has been in operation for 15 years). We believe that substantially better performance can be gained by incorporation of drift chamber technology to supplement the MWPC system.

The MWPC portion of the tracking system consists of 32 planes distributed throughout the 1.5 m height. This array approximates a continuous instrumented volume in front of the magnet. The concept is illustrated in fig. 6. It

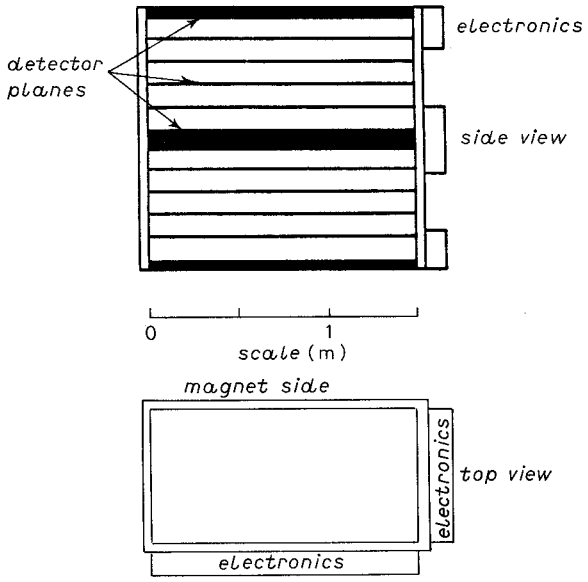

Fig. 6. – Tracking system: mechanical design.

provides for maximum sensitivity to scatterings of particles traversing the field (in order to reject fake antimatter events) and provides good deflection resolution since the entire structure is rigid and has a uniform temperature coefficient. The walls of the volume will be made of NEMA G-10 from top to bottom. Since the tracking system is a rigid structure of uniform composition, it will expand and contract uniformly. An alignment monitoring system will not be necessary. Balloon experience with a system of 1.1 m height has shown that temperature variations at rates of 10 °C/h over the range (10 ÷ 50) °C do not result in detectable mechanical distortions (less that 10 microns change in a particles measured curvature).

Nuclear scattering, Coulomb scattering and Rutherford scattering are all processes to be minimized in a tracking system used for cosmic-ray studies. This is especially true for measurements of antiprotons and sensitive searches for anti-alphas. The WiZard tracking system contains only 0.27 g/cm^2 of material (mostly argon) which is equivalent to 0.014 rad-lengths and 0.002 proton nuclear interaction lengths.

Figure 7 contains a block diagram of the MWPC portion of the tracking system electronics. The electronics is based on the Microplex VLSI integrated circuit developed for silicon strip detectors and now being used in MWPC systems. The axis orthogonal to the magnetic field is the axis on which one observes the curvature. In this axis, each of the 32 planes is serviced by 5 Microplex chips and a readout controller. The Microplex chips are connected to the MWPC cathode wires. Each track appears as charges induced on the cathode wires by the avalanche that occurs on the anode wire. Determination of the particle position is made by finding the center of the induced charge region.

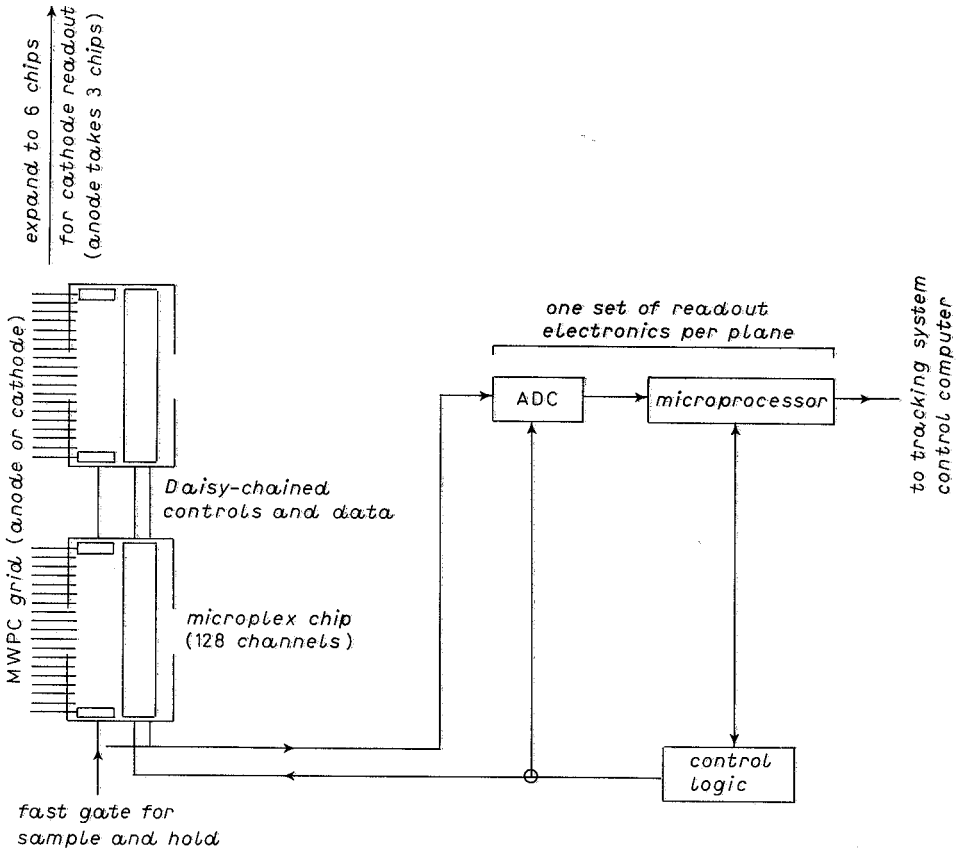

Fig. 7. – Tracking system: electronics.

In addition, the axis parallel to the magnetic field is instrumented with 3 Microplex chips per plane. These chips are connected to the anode wires. In general, only the wire nearest to the track will show a pulse. Data from this axis has lower resolution but it provides simple binary signals which can be used to evaluate whether or not usable tracks are present. The logic will be programmable and will have adjustable selection criteria. Experience with the PBAR experiment and with computer simulations of expected background events indicate that testing for track quality will eliminate over 90% of the triggers caused by cosmic-ray interactions in nearby material (such as the Astromag magnet coil).

A tracking system computer controls the overall event readout. The electronic components are all available in space-qualified or soon to be qualified forms [45]. The Microplex chips consume only 60 mW/chip. The current MWPC system with its distributed delay-line readout has a demonstrated long-term resolution of 125 microns averaged over a zenith angle distribution similar to WiZard's [40]. This system has been shown to have a resolution of 90 microns when used with a better read-out system [46]. For purposes of establishing overall instrument performance we have assumed a very conservative resolution of 100 microns.

The entire tracking system will be filled with the MWPC gas. A cleaning system, composed of a molecular scrubber and a reciprocation system, with 1 volume/day capacity will provide a wide margin of safety for avoiding contamination build-up in the tracking system.

c) Transition radiation detector. The TRD operates on the principle that relativistic particles traversing boundaries between dissimilar media emit radiation induced by the change in the dielectric constant of the media. The TRD proposed here uses precisely manufactured carbon fibers to provide transitions. In this case extreme relativistic particles (with a gamma > 1000 or so) emit X-rays of an energy which can be detected in a MWPC. Electrons and positrons with energies above 500 MeV satisfy this criterion, but protons must have energies above 1 TeV to produce transition radiation. Thus, a $Z = 1$ particle with energy less than 1 TeV that is emitting transition radiation is an electron or positron. The TRD proposed here has 10 layers of carbon fibers each separated by an MWPC. This allows good efficiency, redundancy and detector cross-checks. Each layer consists of the radiator material and an MWPC. The use of carbon fibers allows an overall reduction in the vertical height of the detector. The total amount of material in the TRD amounts to 0.13 radiation lengths and 0.05 interaction lengths.

Readout electronics will employ the cluster-counting technique commonly used in TRDs at accelerator experiments. The cluster counting technique is only sensitive to the narrow MWPC spikes caused by X-ray interactions. These interactions result in extremely localized ion production and thus very narrow

pulses (in the time domain). The signals due to charged particles are distributed through the entire chamber volume and are thus much broader in time. In accelerator experiments it has been found that cluster counting is a much more powerful method than pulse-height for detecting the transition radiation [47]. The use of carbon fibers and cluster counting makes it possible to achieve better performance with single 10-layer counter than one could achieve with two 6-layer counters used in the baseline desing of the Astromag report [45].

The MWPC utilize a Xenon-CH_4 gas mixture supplemented by a recirculation system of the same design as used for the tracking detector, and an on-board gas makeup container.

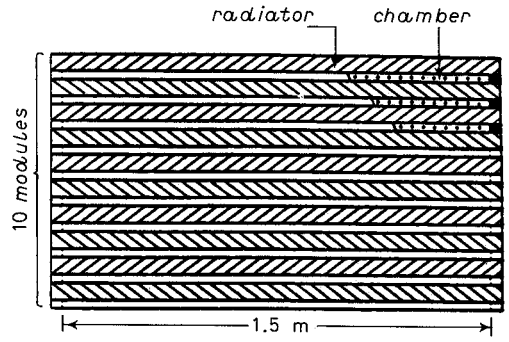

Fig. 8. – TRD mechanical design.

Figures 8 and 9 show the mechanical and electrical schematics for the TRD detector system. The cluster counting electronics on each wire is interfaced by a local data bus to a central TRD read-out computer. The central TRD computer is responsible for collecting the data and preparing the appropriate message for the WiZard main computer. The TRD electronics structure naturally lends itself to parallelism in the data architecture. Thus failures of electronics components result only in a partial loss of detector-sensitive area.

d) Calorimeter. The electromagnetic calorimeter provides WiZard with added discrimination of electrons from protons measuring the energy deposited as particles pass through a high-Z material such as lead or tungsten. Electrons produce photons by bremstrahlung which in turn pair produce to form an electron positron pair, resulting in a shower of particles. The distribution of these particles in the detector has a characteristic form for showers generated in this way. The characteristic scale length for the longitudinal development of this shower is the radiation length (about 3.5 mm in tungsten). In most calorimeters, the high-Z material is alternated with a detector material to sample the growth of the shower. A small fraction of protons will produce a neutral pion early in the detector, which decays into two photons and produces a shower similar to an

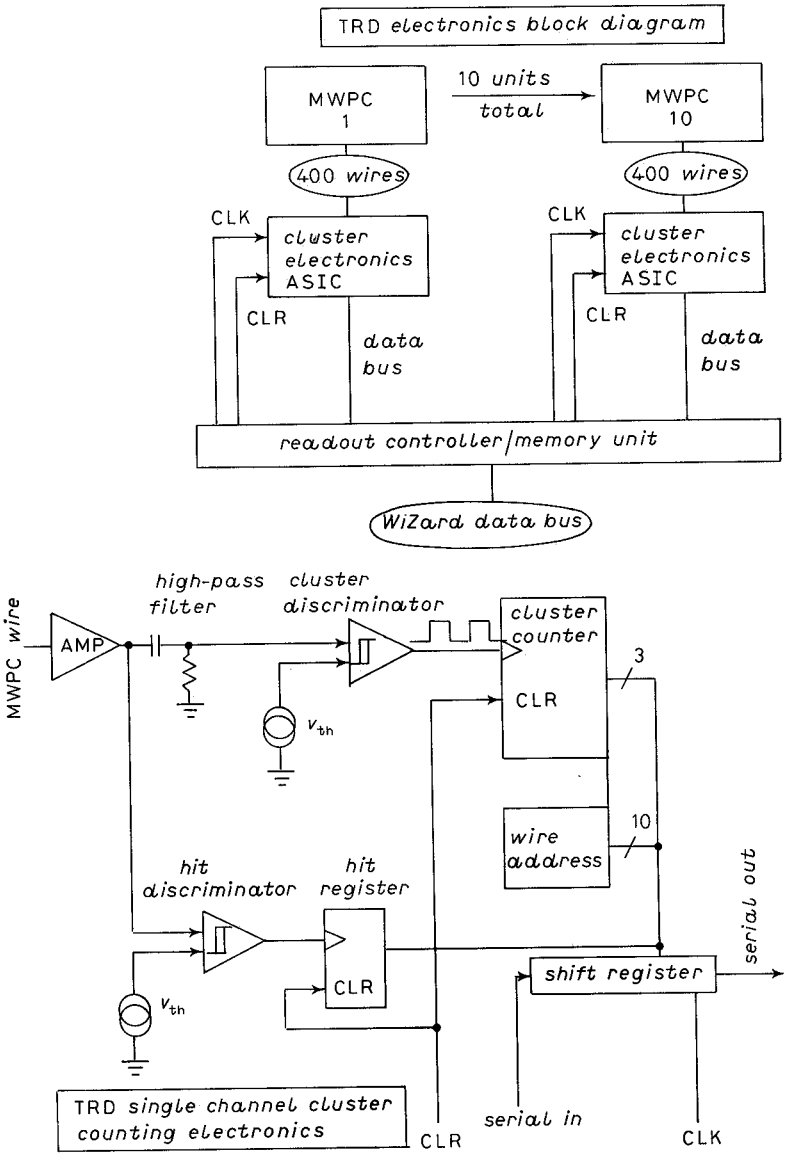

Fig. 9. – TRD electronics.

electron shower. The ability of the calorimeter to discriminate electrons from protons depends on the spatial segmentation of the detector to recognize the difference in development between electron and proton showers. It also depends on the energy resolution of the calorimeter. Good energy resolution allows one to compare the momentum measured in the magnetic spectrometer to the energy deposited in the calorimeter.

The choice of detector medium is critical for high-energy resolution. Low-density detectors, such as MWPCs, suffer from two types of fluctuations not important in higher-density detectors [48]. Because of the small amount of matter involved, Landau fluctuations in the energy deposit for each electron are important. In addition, MWPC calorimeters are subject to pathlength fluctuations due to the large number of low-energy electrons which can move along the MWPC layers (perpendicular to the shower axis) and thus be weighted heavily in the sample due to their long pathlength in the MWPC. The overall degradation in resolution is a factor of 2-3. Scintillator is not subject to these fluctuations, but complex lightpipes and a large number of photomultipliers are required. A

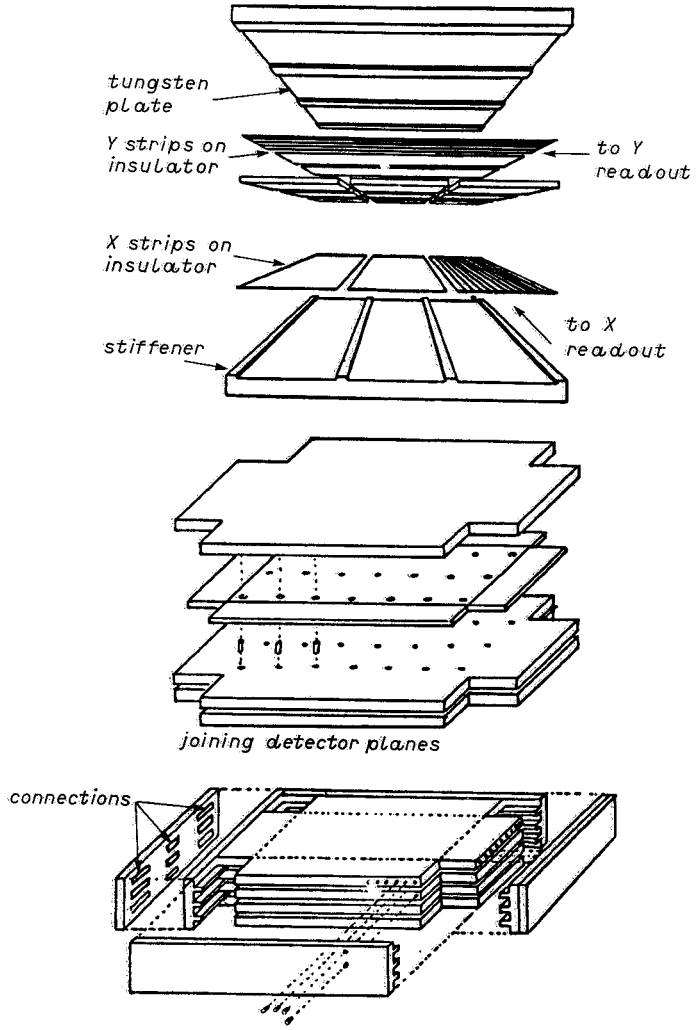

Fig. 10. – Calorimeter electronics.

suitable dense detector material for WiZard is silicon, which has been flown in space since the 1960's and is in wide and rapidly growing use in the high-energy physics community [49]. It is now possible to construct arrays of silicon wafers configured to act as small (4 mm square) particle detectors. Such silicon planes have significantly better dynamic range than MWPCs, which saturate in the dense regions of the shower core. They are simple, requiring no high voltages or gas system. Readout electronics for these detectors is simple and low power, based on the same Multiplex VLSI circuit mentioned in the tracking system.

Figure 10 shows the mechanical assembly of the silicon detector. The calorimeter will consists of 25 layers (each of $0.4 X_0$). Each layer will include a tungsten sheet, an array of silicon wafers, two layers of insulated conductor strips and a stiffening plate. Electrical connections to the silicon are made via 4 mm wide conductor strips printed on the insulation layers. The top and bottom layers are orthogonal, forming 4 mm square read-out pads. Contact between the strips and the silicon is made using a conductive bonding agent. The 25 layers are pinned together and mounted in a structural housing that also incorporates the electronics.

e) WiZard *electronics*. Figure 11 shows a block diagram of the WiZard electronics. As mentioned earlier, triggering of the instrument is by a fast coincidence from the TOF counter. This signal is given to each of the detectors

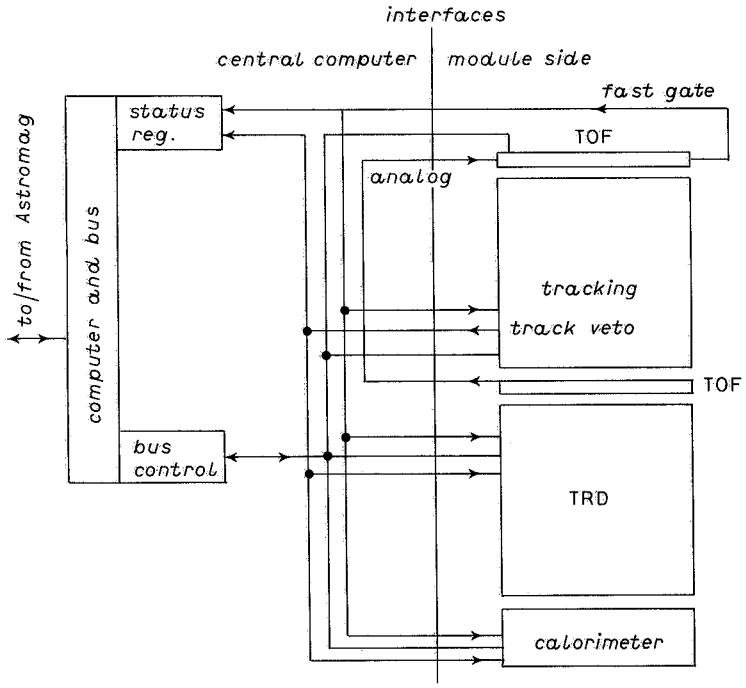

Fig. 11. – Calorimeter mechanical design.

and to the central computer. The signal is used by the individual detectors to initiate their digitizing sequence. A slightly slower signal is developed by the tracking system (see the preceding section on the tracking system). This signal is asserted if the proper track measuring criteria are not met. It is used as a reset for the detectors. The central computer is also notified. Each module is required to perform its own signal processing including conversion of the signals to digital information. This information is then gathered by the central computer via the instrument data bus. The central computer concepts of onboard processing and event selection are based on a similar system used in the NASA/NMSU BBMF.

Two computers with redundant interfaces will act as a redundant central computing facility. Selection of the primary computer of the pair will be made by command from the ground. The system will be designed so that central controller malfunctions cannot produce safety hazards or hazards to the detectors. Failure of a central computer will be detected by failure of internal consistency checks embedded in the data or by failure of periodic self-test. Since lost of a central computer only results in loss of observing time, a relatively slow reaction time can be easily tolerated. The cost savings of this approach to redundancy are considerable when compared to a majority voting technique.

The WiZard backbone also provides the Astromag signal and power interfaces, and low-voltage power supplies for the entire apparatus. The detector modules have been designed with a high degree of autonomy. This allows dramatic simplification of the interfaces between the modules and the backbone facility. These interfaces can be constructed inexpensively but in such a manner that they can be mated and de-mated on-orbit. Since they will be mated before launch, no connector operations other than the connection to Astromag will be required for the two-year duration of this experiment.

f) Mechanical assembly. Figure 12 shows the instrument mechanical assembly. Individual instrument modules are integrated into the backbone structure which is also used as the shuttle launch carrier. The design provides, however, for the delivery of the initial instrument as an integrated package. This is to simplify the crew requirements for installation and to eliminate the necessity of Astromag providing «universal» robotic-compatible interfaces for each detector module. The instrument is designed to be capable of determining the relative locations of all of its modules as well as the location of the magnet by using cosmic-ray information alone. This feature eliminates the need for high-precision alignment during assembly and during installation at Astromag. It is a well proven technique, having been routinely used by the NASA/NMSU BBMF for 15 years. A modular approach was chosen for the detector systems in order to simplify the integration of the payload and to support the possibility of change-out of modules to conduct new experiments in the future. Accommodation of on-orbit change-out of detectors without major increases in cost and complexity is not an easy matter. We propose to include such studies in our Phase 1 effort.

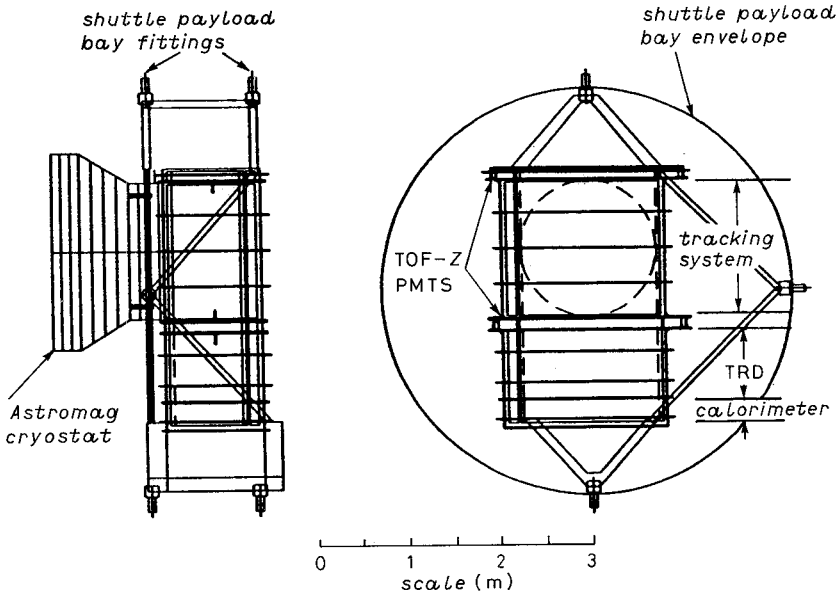

Fig. 12. – WiZard electronics block diagram.

g) Interface with the Astromag core facility. The interface with the Astromag core facility can be made via a standard Space Station attached payload fixture. The interface requires mechanical and electrical connections but no active thermal support. Location of the instrument relative to the magnet face with an accuracy of 0.5 cm is quite sufficient. This is because our instrument is capable of determining the magnet location directly from the cosmic rays themselves. The instrument uses standard space station 208 V power and creates its own internal regulated voltages. The data interface will be in accordance with the Astromag standard serial data bus.

2·2. *Performance characteristics.* – In this subsection we present the expected performance of the WiZard instrument. The performance is discussed in the context of each of our observational objectives. Our performance estimates are based of actual performance of existing systems supplemented by Monte Carlo calculations. The Monte Carlo calculations fall into two categories: 1) simulation of specific detector responses using programs specifically written to simulate that detector's function, and 2) simulations using the GEANT particle interaction program. GEANT is a program which was originally devised as a design tool for developing large-particle detectors at CERN. It is now a de facto standard for design of all large-particle detection experiments. It allows the designer to incorporate a mathematical model of the proposed detector system and study its response to bombardment from any angle by any type of

particle. The programs have been checked for accurate performance by direct comparison of simulated data and actual data gathered with similar instruments.

a) Rigidity resolution. Figure 13 shows the MDM *vs.* geometry factor for the instrument. This distribution is based on an assumed 100 μm resolution for the individual tracking system planes. Note that a significant portion of the

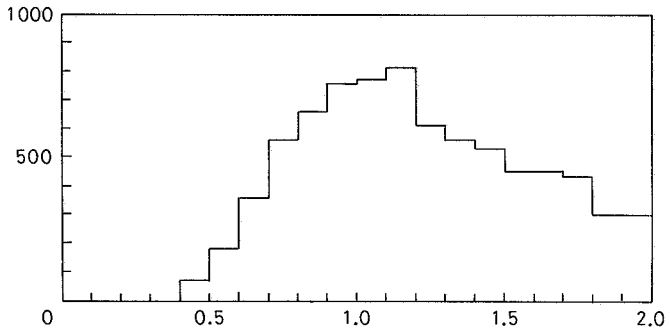

Fig. 13. – WiZard mechanical assembly.

tracks have resolutions greater than 2 TeV. We have found in the past that energy spectra measured with a momentum spectrometer are usable up to the 1/2 of the maximum resolvable rigidity. Thus this experiment should be capable of measuring energy spectra from geomagnetic cut-off to at least 1 TeV. It should be noted that this performance is based on the extremely conservative assumption of 100 μm resolution in the spatial detectors. Inclusion of higher resolution drift chamber technology may well result in doubling the upper energy limit of the system.

b) Detection of antinuclei. Performance of the instrument as a detector of anti-helium depends on three factors. First, the TOF must clearly separate upward from downward particles. The Earth helps, acting as a shield, for upward going particles but at lower energies particles can mirror below the space station. One must also be able to demonstrate that there are no albedo particles from the Earth's atmosphere as well. As discussed in the TOF discussion above, the TOF provides 20 standard deviations between upward and downward moving particles. The second factor is that the tracking system must determine the correct sign of curvature. We have performed extensive studies based on Monte Carlo calculations that included Coulomb scattering, small-angle coherent nuclear scattering and measurement error. (This analysis is similar to that used to calculate the curves in fig. 14 of the next section.) The analysis shows that the expected rate for spurious anti-alphas is far below 10^{-8} for energies from geomagnetic cut-off to 50 GeV. The principal reasons for the low spurious event rate are: 1) the large number of spatial measurements (effectively

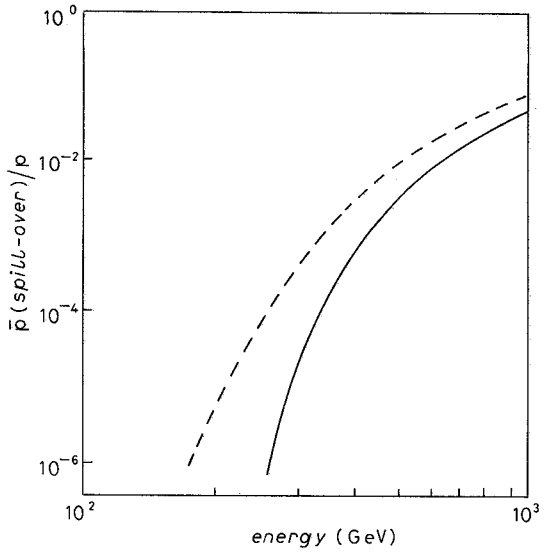

Fig. 14. – Antiproton background from spill-over protons: —— resolution cut at 1 TV, --- resolution cut at 0.7 TV.

eliminating the chance of scatter-events of fitting), and 2) the very low amount of mass in the tracking system (which makes the total number of scatter events small). As mentioned earlier charge resolution must also be considered. There are negatively charged particles with charge = 1 traversing the instrument (electrons, antiprotons and a few mesons). These must not be mistaken for charge = 2 or greater. To eliminate this possibility we will utilize pulse-height measurements from the TOF, and tracking systems. Additional pulse-height data from the TRD and calorimeter will be available for further cross-checks. The $Z = 1$, $Z = 2$ overlap will be substantially less than 1 part in 10^8. One also worries about pathological events such as unusual charge exchange collisions, odd combinations of multiple-particle events, etc. Using GEANT, we have found that requiring every detector to have both tracking and pulse-height measuring capability allows one to develop a complete picture of each event. Events that would indeed be pathological in less capable detectors are cleanly eliminated in our system.

c) *Antiproton measurements.* The detection of antiprotons requires reliable recognition of particles with a charge of -1. This involves time-of-flight measurements (discussed earlier) and measurement of rigidity. The possible particles with charge = -1 are electrons, antiprotons and mesons (pions, muons and kaons). One should also consider the possibility of protons appearing to have negative curvature due to scattering or simply measurement error. Separation of antiprotons from electrons is easily accomplished in a system that must also separate positrons from protons. This separation is discussed in great detail in

the next paragraph. In this section we address the remaining problems of antiproton detection.

Figure 14 shows the expected spill-over of protons to the negative curvature regime. The predominant source of spill-over events is the measurement error. We have also incorporated Coulomb scattering and small-angle nuclear scattering into the simulation. Because of the low mass in the tracking detector and the large number of measured points along the track, the scattering contributions to the spill-over are negligible. From fig. 14 it can be seen that the antiproton flux will be measurable up to 300 GeV/c or so.

For balloon experiments, the most troublesome background in antiproton experiments is the μ^- and π^- produced in the atmosphere above the payload. Although locating the experiment in space does eliminate the atmosphere, there are other masses in the experiment and located nearby that can act as sources of meson background. For WiZard we handle the problem by trying to minimize the possibility of undetected meson production. We have also devised schemes for testing for the presence of the background. From the design standpoint, we have reduced to a minimum the amount of material in the entrance aperture and the tracking system. We have also instrumented the volume traversed by the cosmic rays as much as possible with both tracking and pulse-height sensors. This instrumentation makes it extremely unlikely that interactions could occur undetected.

The design options have been carefully considered using the GEANT program to search for possible sources of fake antiproton events. We propose to continue refinement of the design using GEANT during the Phase-1 effort. Several cross-checks exist in the WiZard experiment to further test the validity of our antiproton measurements. First all of the processes for production of background meson contamination are strongly peaked at low energy. Such background should also appear as a flux of antiprotons whose energies appear to be below geomagnetic cut-off. At higher energies it is possible to verify the mean mass of the antiproton candidates by utilizing the multiple measurements of $\mathrm{d}E/\mathrm{d}x$ in the tracking system. These measurements should have sufficient resolution to detect the relativistic rise in ionization should mesons be present in the energy range $(10 \div 200)$ GeV.

d) Observations of electrons and positrons. The observation of spectra of e^- and e^+ requires some form of identifying particles of low mass. Positrons are the hardest to measure because the proton/positron ratio is around 10^4. Thus to measure positrons reliably, one must have a system which has a probability of mis-identifying a proton as a positron which is significantly lower than 10^{-5}. To accomplish this objective we employ both the TRD and the calorimeter. As mentioned earlier the TRD utilizes the cluster-counting technique to obtain the best possible distinction between electrons and protons. Figure 15 shows the expected response of the TRD as function of the particle's relativistic time

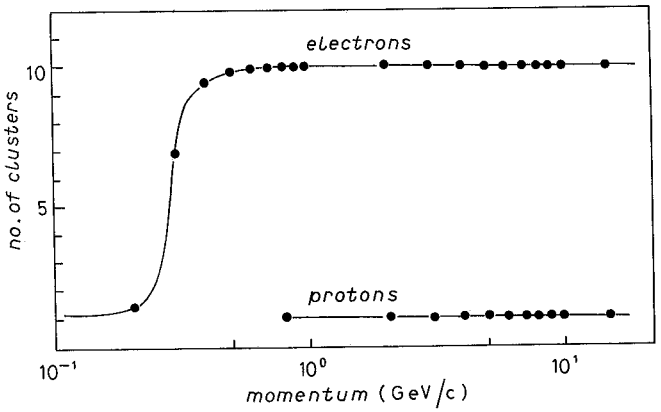

Fig. 15. – TRD response to electrons and protons.

dilation factor (gamma). When a particle is fully relativistic it will produce an average of one cluster per layer in the 10 MWPC planes. Figure 16 shows the probability distribution of electron and proton cluster counts. The figure is based on the Monte Carlo technique described in [50] and was generated using 10^5

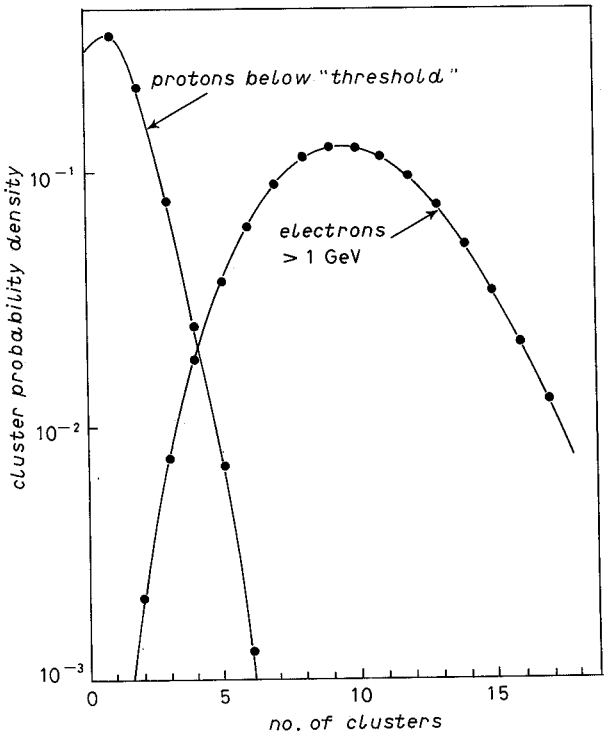

Fig. 16. – TRD cluster count probability distribution.

events. The curves are applicable to cases where the proton is below the TRD threshold (about 800 GeV) and the electron has an energy above 1 GeV. From fig. 16 we conclude that if one uses the TRD as a 90% efficient detector of positrons, it will falsely identify 0.2% of the protons as positrons. If one uses the TRD as a 90% efficient detector of antiprotons, it will falsely identify 0.35% of electrons as antiprotons.

The calorimeter allows discrimination between electrons and protons by starting-point, shower energy, depth of shower maximum and shower width. In the past calorimeters employed infrequent sampling of the shower growth and crude (or nonexistent) lateral sampling. Typically these systems gave electron/proton separations of around 10^{-2}. The calorimeter in the WiZard experiment performs 25 samples in depth. It also has excellent lateral segmentation and total energy measurement capabilities. We have made extensive GEANT simulations of both electron and proton cascades in the calorimeter. Figure 17 shows average growth curves for shower energy (*i.e.* energy deposited in each layer) and shower size (*i.e.* a mean width of the ionization) as a function of depth

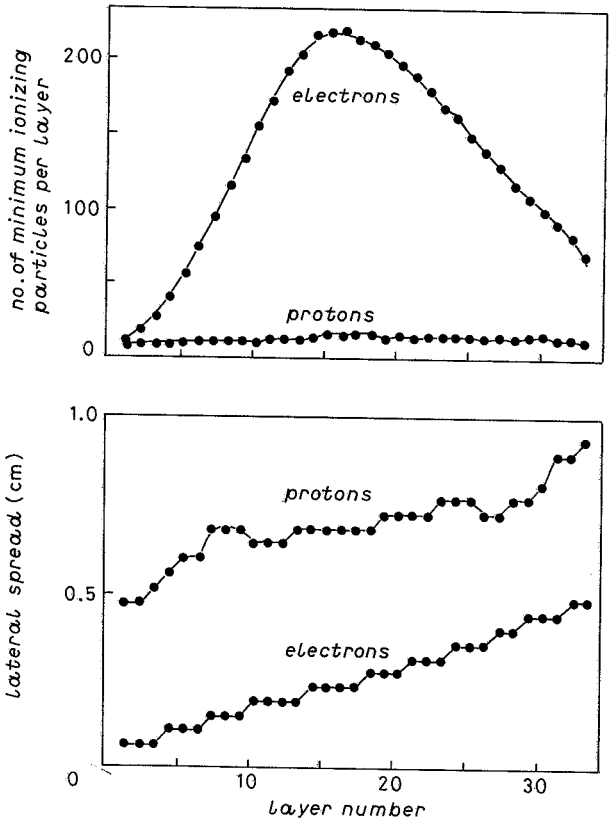

Fig. 17. – Silicon detector response *vs.* layer (at 20 GeV).

for 20 GeV incident particles. (The proton curves include the requirement that the proton have an interaction in the first 4 radiation lengths.) Using information from GEANT simulations, it is possible to parametrize the likelihood function as a function of energy using all of the above information. To test a given cascade, the 25 measured energy depositions and the 25 measured shower widths are used (together with the knowledge of the particle's rigidity) to construct a likelihood for the two hypotheses (electron or proton). The likelihoods are then used to decide the particle's identity. In preparation for this proposal 2000 proton and electron showers have been simulated (by GEANT) at energies of 10, 20, 50 and 100 GeV. At all energies, the electron recognition efficiency was above 97% while no protons were observed to survive the same selection. We conclude that the misidentified proton error rate is consistently below 10^{-3}.

Note that the calorimeter and TRD discriminations are completely independent. Thus we can multiply the two discriminations together to get overall system performance. At high energies, the combined discrimination power gives an expected fraction of protons appearing as positrons of less than $2 \cdot 10^{-6}$.

2·3. *Observing plan.* – The observing program will begin with experiment wakeup and checkout. This period will require that the magnet be turned off. About one week will be reserved for checkout of individual detectors and operation of the instrument as a whole. Calibration data will be taken at the end

TABLE II. – *Required observing times for various objectives.*

Species	R_{max} (GV)	Period (*)	Science objectives
Primary			
p	1500	< 1 day	acceleration, propagation, spectral universality etc.
He	1500	1 week	
C	1000	2 weeks	
up to iron	1000	2 to 8 weeks	
Secondary			
Li	1000	1 y	propagation, re-acceleration, etc.
Be	1000	3 y	
B	1000	1 y	
Antiprotons	300	20 weeks	closed Galaxy, sources, etc.
Antiprotons	250	2 y	dark matter, leaky-box model, extragalactic antiprotons, etc.
Electrons			
e^-	1000	2 y	physical conditions in the acceleration and propagation sites, etc.
e^+	400	2 y	origin, propagation, dark matter, signature, etc.

(*) Based on 50 particles to be observed between $0.8\,R_{max}$ and R_{max}.

of this period to establish baseline pulse-heights, noise rates, spectrometer alignment and location of the detectors with respect to the tracking system. Calibrations will be taken for at least a week to determine system stability. When the Astromag facility is ready, the magnet can then be charged and initial data aquisition can commence. The instrument will be configured for our prime objectives at this time. Table II shows the observing time required for various objectives. Figure 18 shows the numbers of particles/week gathered by instrument above a given rigidity.

Note from fig. 18 that one week of observation allows measurements of all species up to at least 100 GeV/c. During the same week over $3 \cdot 10^6$ alpha particles will be measured. Just this one week will represent a significant improvement in the amount of data available to address the key scientific issues

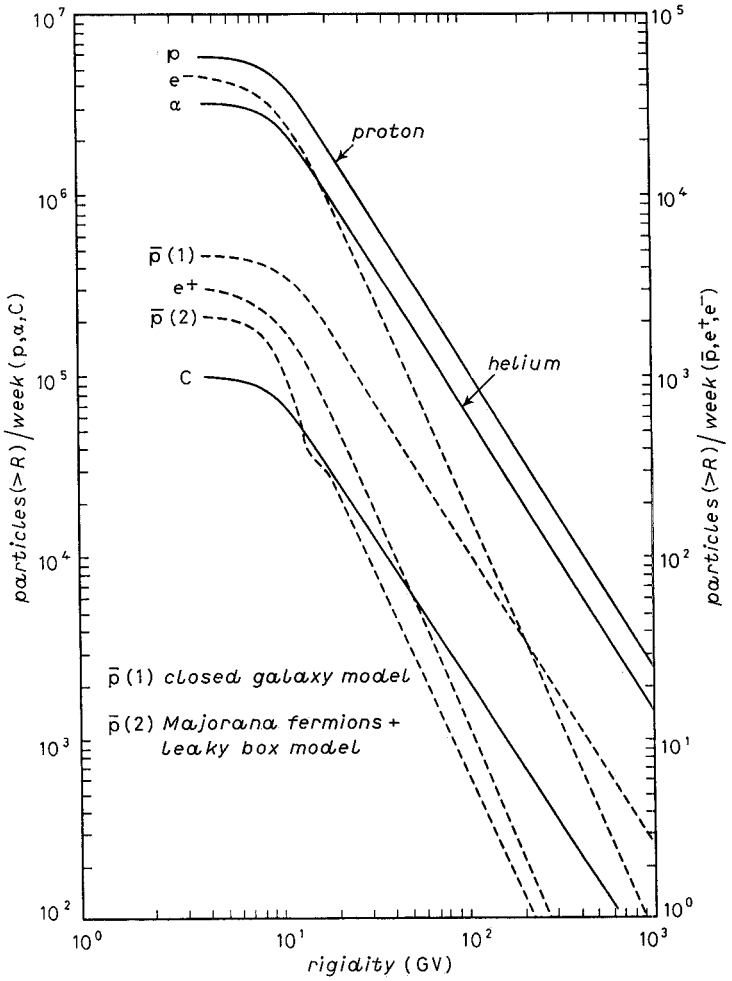

Fig. 18. – Number of events/week.

outlined in sect. 1. Because the data is so important the initial publication effort will begin with the aquisition of the first week's data. WiZard data aquisition will continue in parallel with this initial publication effort.

Overall experiment alignment and stability will be monitored by taking advantage of the many redundancies with the basic data. Experience with the NASA/NMSU BBMF balloon payload indicates that that the spectrometer alignment is stable for periods well in excess of 6 months. Periodically we will request that the magnet be turned off, if Space Station operations do not impose such periods frequently enough. During these periods the calibration baselines will be re-established and compared to past calibrations to establish limits on calibration drift rates. Interruptions in magnet-on observing periods are of minor consequence. They simply reduce the overall observing time.

When the primary observing goals have been reached, the instrument will be operated in a mode which optimizes observations of heavier nuclei. During this period a survey of the energy composition (and antimatter content) of nuclei from carbon-iron will be studied. At the end of this period the instrument will be made available to NASA to be used by other investigators for other objectives.

2·4. *Instrument integration.* – The instrument is constructed of detector modules connected to a backbone structure which incorporates the central computer and low voltage power supplies. Each element in the system is designed with a high degree of autonomy. Mechanical and electrical interfaces are designed to be as simple as possible. The backbone structure will also serve as the payload carrier.

The backbone and each instrument module will incorporate their own self-test, diagnostic and housekeeping functions. Prior to delivery to the system integrator, each module will have passed its own performance and qualification tests. The modules will then be assembled into the backbone. Initial form, fit and function tests will include verification of performance using atmospheric cosmic rays. If a full scale Astromag coil is available, these tests will be made with that magnet. If the Astromag coil is not available, the NMSU 0.67 m magnet (which is almost exactly half scale) will be used. Tests during this phase of integration will include: magnet-off tests:

1) Verification of spectrometer alignment.

2) Verification of tracking system resolution magnet-on tests.

3) Verification of trigger performance.

4) Verification of each detectors performance.

5) Verification of the particle identification schemes.

Once the form-fit-function and science checks are complete, the instrument will be delivered to GSFC for formal payload integration testing.

2·5. *Ground operations.* – In this subsection we describe support required and proposed science activities the in various phases of ground operations:

2·5.1. Pre-launch. Operation of the instrument for verification of function and recalibration will be performed as needed during payload integration testing. These operations will utilize atmospheric cosmic rays as their signal source. From the time of completion of the integration tests until the beginning of on-orbit operations the payload can remain unpowered and inert. Occasional power-ups or partial power-ups to perform status monitoring can be supported. The frequency and duration of these operations will be determined in response to more detailed flight operations planning.

2·5.2. Post-launch. No special operations will be required other than those mentioned elsewhere for the WiZard ground data systems.

2·5.3. Related particle-accelerator activities. Accelerator studies are required for all the detector systems. In the case of the TRD one needs to i) determine the detector threshold and the growth curve for transition radiation, and ii) evaluate the efficiency and the discriminating power for electrons. The calorimeter needs to be tested for i) the energy calibration, ii) its discrimination ability between protons and electrons, and iii) the granularity requirements for read-out and signal processing. These studies have to be carried out to an accuracy such that the uncertainty in the discriminating power is much smaller than the statistical errors associated with the WiZard measurements. In the case of the tracking system it is essential to i) determine its resolution and ii) evaluate the requirements to record tracks efficiently from relativistic protons to iron nuclei. The ability of TOF system to distinguish between a relativistic proton and a helium nuclei at a level of one part in 10^6 needs to be examined for different incident angles and locations.

2·6. *Flight operations.*

2·6.1. Science activities during flight. Figure 19 shows an overview of the WiZard data system that will be used to support the flight science activities. The real-time aspects of WiZard flight operations will be performed by the WiZard command/control center (WC^3). Monitoring of experiment science performance, calibrations etc. will be performed at NMSU in a near real-time mode operating via computer-link to the WC^3. Output of WC^3 will be in the form of level-0 data, ephemerides, housekeeping data, and an event log. This output will be delivered to the WiZard processing center where it will be made available to the WiZard science team via the science team network. The WC^3 will be responsible for monitoring redline parameters and executing short-term experiment control. The general execution of the observing plan will be in accordance

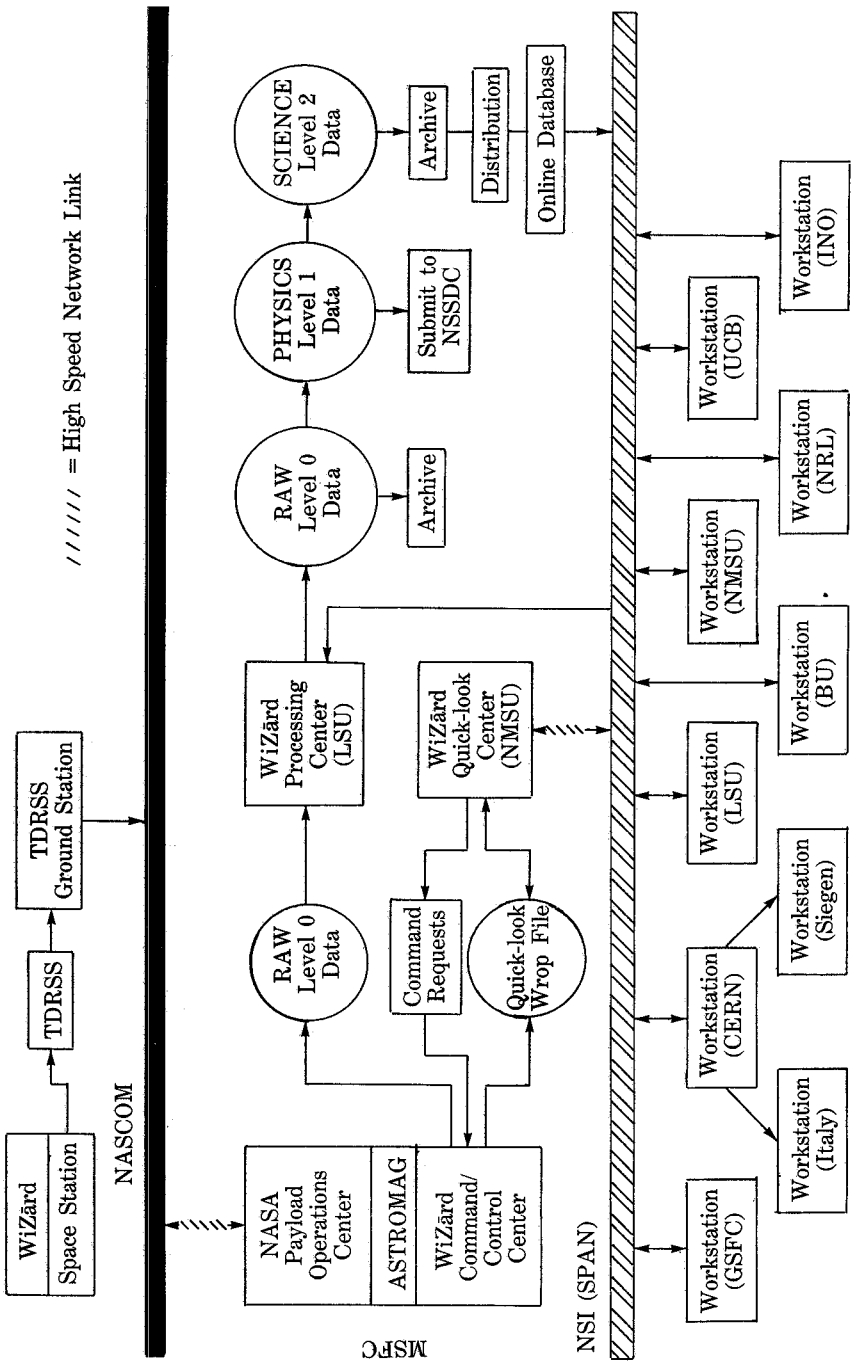

Fig. 19. – WiZard data system.

with directions given from NMSU based on quick-look analysis and science team inputs. Longer-term scientific operations planning will be based on off-line analysis made by the science team using the WiZard processing center as a source of processed data.

2·6.2. Mission planning.

2·6.2.1. Operational constraints. – There are no operational constraints except those noted in the viewing requirements.

2·6.2.2. Viewing requirements. – In general, the instrument must only be pointed away from Earth. Pointing within 45° of the zenith would be more than adequate. It should be noted that interpretation of the data will require knowledge of the aspect angles with a few degrees accuracy. No massive objects can be permanently mounted so as to obscure the area within 45° of the instrument vertical axis. Transit of such objects through the field of view is acceptable provided such events are logged by the WC[3].

2·6.2.3. Pointing requirements. – See previous paragraph.

2·6.2.4. Communications needs. – The WiZard instrument will normally operate at a maximum 35 kbit/s downlink data rate. Occasional use of up 250 kbit/s is desirable to support calibration and diagnostic modes of operation. The 250 kbit mode should constitute less than 3% of the observing time. Commands will be only occasional (less than 1% of observing time). Command data rates of 9.6 kbits/s would be acceptable. No special communications facilities are required. The flight system interfaces and ground interfaces will all conform to normal Space Station standards.

2·6.2.5. Tracking needs. – Ephemerides are needed to 5 n.m.i. accuracy. They are not needed in real time.

2·6.2.6. Special techniques. – No special techniques, EVA or control thruster restrictions are needed during instrument operation.

2·6.2.7. Orbital requirements. – No special orbital requirements are needed with regard to time of day/month, moon phase or lighting conditions.

2·6.2.8. Real-time ground support requirements. – The WiZard experiment will need no additional support other than that normally provided by the Space Station attached payloads operations center and WC[3].

3. – Data reduction and analysis.

3·1. *Organization overview.* – The size and composition of the WiZard science team was largely driven by the understanding that data analysis and timely publication of WiZard data will be perhaps the most challenging part of the project. The objective of the entire WiZard program is the production of publications and data for the NSSDC archives. The amount of data to be produced by the WiZard program is large enough that very special care must be taken to assure that it is recorded and analysed efficiently. We have found it a significant challenge to reduce the data from even 1 day's flight (2 gigabytes of data) from the BBMF balloon payload. To effectively deal with 2 years of data at 4 times the rate we have to be very innovative.

Our strategy in meeting this challenge is twofold. First, we intend to make heavy use of preprocessing and event selection. The process is described in detail later in this section. Preprocessing and event selection have the advantage of reducing the size of the data set and increasing analysis speed. In order to minimize the risk of operating with inappropriate on-board processing and selection, the on-board system will pass on small sample of unprocessed data so that ground verification of the flight processing can be performed in near real time. The on-board processing and selection criteria will be under command control. These techniques have been applied in recent balloon flights with very satisfactory results.

A second part of our data-handling strategy lies in distributing the analysis tasks amongst the members of the collaboration. Our concept for the off-line analysis and processing utilizes a central processing facility supplemented by institutional computing facilities. Figure 19 shows an overview of the WiZard data system. The institutional facilities will be networked to the central facility. This architecture will allow parallel efforts such as individual detector calibration studies but still focuses publication related work through coordinated use of the central facility. This architecture will allow parallel efforts such as individual detector calibration studies but still focus on publication-related work through coordinated use of the central facility. Individual institutions will carry forth their assignments on their own computing facilities to the maximum extent possible (background studies, calibrations for individual detectors, etc.). The central processing facility will be the source of level-2 data to support these efforts. The PI, acting with the advice of the science team will coordinate the activities of the institutions and the central processing facility. During the two-year observation period, the priority of activities will be: 1) verification of payload function, 2) analysis for publication. As mentioned earlier, some results will be published early in the flight. The final publications will appear one year after completion of the observing period. The WiZard team has already considered the matter of publication rights. These rights will be established as part of the contracts and memoranda of understanding between NMSU and the

science team members. The basic principal in the publication rights will be that any publications based on the level-2 data will have the entire science team as coauthors.

3·2. *Onboard processing.* – If all the raw data from every trigger were transmitted to the ground, WiZard would require a real-time data rate in excess of 350 kHz. Fortunately the data from the WiZard detectors is quite sparse. Data from portions of the detectors where a particle did not pass is of little interest so it is not generally necessary to transmit all available data. Each detector module incorporates its own computer system in order to gather the significant data and provide reduced data to the central WiZard computer. The central computer is also capable of categorizing events in real time. Most of the triggers will be either due to side showers caused by interactions of cosmic rays with nearby material, and low-energy protons. The side shower events will in general not transmitted. For events such as low-energy protons only a brief report (charge, rigidity etc.) need be transmitted. The result is a reduction by a factor of 10 in the data transmission rate without degradation in the physics. In order to assure that the selection of events for transmission is functioning properly, a fraction of such events will be transmitted with full information. Occasional diagnostic runs will be made in which full information on every event is transmitted.

3·3. *Ground processing (real time and quick-look).* – The WiZard command and control facility (WC^3) includes a MicroVAX processor with appropriate displays, recording peripherals and network communications. Experiment health parameters (temperatures, pressures, voltages etc.) will be monitored at WC^3. WC^3 will issue commands to maintain the desired experiment operating conditions. WC^3 will also perform rapid response commands for experiment «emergencier» and Space-Station operations requirements. The WC^3 will be co-located with the Astromag Control Center.

Quick-look analysis will be performed at NMSU. When commands are desired to maintain optimum science performance they will be made by NMSU request to the WC^3. It is important to realize that rapid response commands are not generally needed to maintain science quality. Except for equipment failures, the instrument performance will change only slowly during the flight. The longer-term aspects of payload operations such as observing plans and overall instrument configuration will be controlled by the science team. These considerations will be forwarded to the instrument operators by the PI.

3·4. *Ground processing (for archive and publication).* – There will be a major central processing facility which will be the repository of the flight data, calibration data, and the collaborations basic software libraries. This facility will contain two types of software: 1) routines for production of processed data, and

2) utility routines for display generation and nonproduction computation aids. Production software will be maintained under strict configuration management. Utility software will be maintained using less strict controls. The central processing facility will be closely coupled to the collaborators institutions via the SPAN network. A secondary facility (to speed distribution of data in Europe) will be located at CERN.

Each institution will have its own analysis/workstation system to perform the following tasks:

Communicate with the rest of the collaboration.

Access the central facility for software and data exchange.

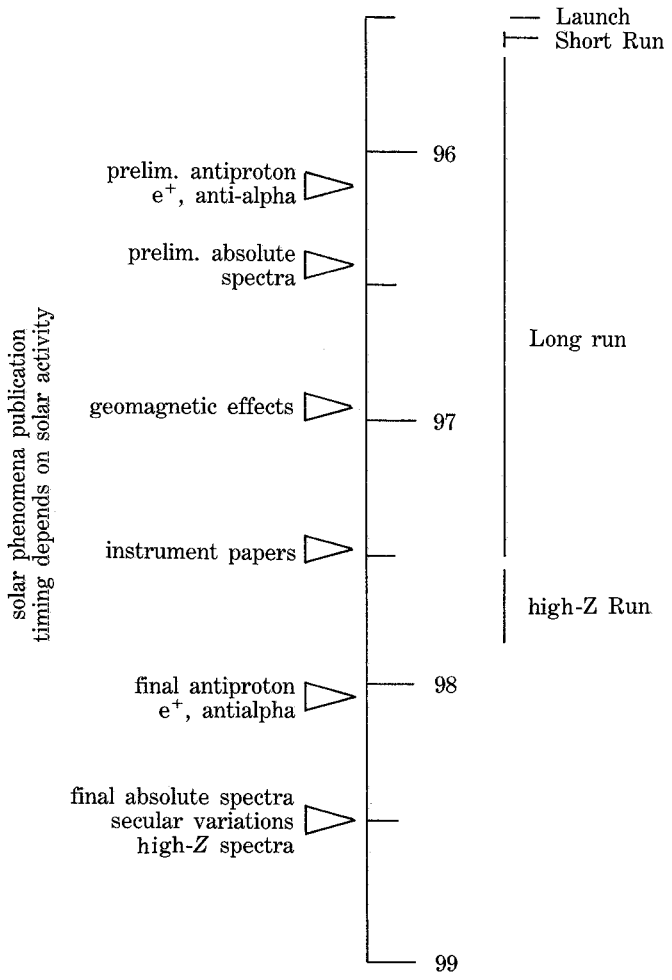

Fig. 20. – Observations and related publications schedule.

Access the central facility for purposes of executing jobs at the central faciliting.

Performing local data analysis tasks.

Development of software contributions to the central facility libraries. Items for the strictly controlled portions of the library will be produced in accordance with the requirements of the software configuration management plan.

Reporting and documentation.

3·5. *Format.* – Level 1 data (processed and calibrated in engineering units) data will be delivered to the NASA archives at the NSSDC.

3·6. *Schedule of science activities.* – Figure 20 shows the major events in the observing program and publication schedule.

4. – Orbiter crew and/or payload specialist training.

Crew involvement will be limited to transferral of the instrument from the shuttle to the Astromag facility. Deployment of the instrument will consist of removing the carrier from the payload bay and placing it in position in front of the magnet face. The carrier is designed for installation using the Shuttle and Space Station remote manipulator systems. The electrical connection will be a single, multi-lead connector. Once the instrument is in place on Astromag, it will be operated through the ground payload operations control center. No further crew support is required for the duration of the experiment.

The installation activities would follow the following agenda:

1) Verify Astromag magnet is off.
2) Open Astromag micrometeroid/safety enclosure.
3) Remove instrument carrier from Shuttle.
4) Transfer instrument to Space Station RMS.
5) Move instrument to Astromag.
6) Position instrument to be latched to Astromag.
7) Perform and verify latching and electrical connection.
8) Close Astromag enclosure.

The installation operation should be somewhat simpler than a satellite deployment from the shuttle but may take longer due to step 5 above. We have given below a summary of the crew support requirements. We have nominally

assigned the transfer to Mission Specialist although any crew member could be easily trained to the tasks.

4·1. *Commander.* – No support required.

4·2. *Pilot.* – No support required.

4·3. *Mission specialist* no. 1 (*in shuttle*).

4·3.1. Task duration. One hour. Mission specialist no. 1 would remove the instrument from the payload using the shuttle RMS and participate in the transferral of the instrument to the Space RMS.

4·3.3. Training. Training would be required for the removal of the instrument from the payload bay and positioning it for transfer. The instrument will incorporate standard grapple fixtures and trunion release mechanisms.

4·3.2. Equipment. Payload bay RMS.

4·4. *Mission specialist* no. 2 (*on Space Station*).

4·4.1. Task duration. Four hours. Mission specialist no. 2 would receive the instrument from the shuttle RMS and then perform tasks 4-8 using the Space Station RMS.

4·4.2. Equipment. Space Station RMS.

4·4.3. Training. Training would be required for the transfer of the instrument and installation in Astromag. The instrument will incorporate standard grapple fixtures and trunion release mechanisms.

REFERENCES

[1] G. F. SMOOT, A. BUFFINGTON and C. C. ORTH: *Phys. Rev. Lett.*, **35**, 258 (1975).
[2] G. D. BADHWAR, R. L. GOLDEN, J. L. LACY, J. E. ZIPSE, R. R. DANIEL and S. A. STEPHENS: *Nature*, **274**, 137 (1978).
[3] R. L. GOLDEN, S. HOREN, B. MAUGER, G. D. BADHWAR, J. L. LACY, S. A. STEPHENS, R. R. DANIEL and J. E. ZIPSE: *Phys. Rev. Lett.*, **43**, 1196 (1976).
[4] E. A. BOGOMOLOV, N. D. LUBYANAYA, V. A. ROMANOV, S. V. STEPANOV and M. S. SHULAKOVA: *Proceedings of the XVI International Cosmic Ray Conference*, Vol. 1 (Kyoto, 1979), p. 330.
[5] S. A. STEPHENS and B. G. MAUGER: *Astrophys. Space Sci.*, **110**, 337 (1985).

[6] S. RUDAZ and F. W. STECKER: *Astrophys. J.*, **325**, 16 (1988).
[7] S. A. STEPHENS and R. L. GOLDEN: *Space Sci. Rev.*, **46**, 31 (1987).
[8] S. A. STEPHENS and R. L. GOLDEN: *Astron. Astrophys.*, **202**, 1 (1988).
[9] J. NISHIMURA, M. FUJI, T. TAIRA, E. AIZU, Y. NOMURA, T. KOBAYASHI, K. NIU, A. NISHIO, R. L. GOLDEN, T. A. KOSS, J. J. LORD and R. J. WILKES: *Astrophys. J.*, **238**, 394 (1980).
[10] R. L. GOLDEN, B. G. MAUGER, S. NUNN and S. HORAN: *Astrophys. Lett.*, **24**, 75 (1984).
[11] T. T. TANG: *Astrophys. J.*, **278**, 881 (1984).
[12] J.L. FANSELOW, R. C. HARTMAN, R. H. HILDEBRAND and P. MEYER: *Astrophys. J.*, **158**, 771 (1969).
[13] A. BUFFINGTON, S. M. SCHINDLER and C. R. PENNYPACKER: *Astrophys. J.*, **248**, 1179 (1981).
[14] R. L. GOLDEN, S. A. STEPHENS, B. G. MAUGER, G. D. BADHWAR, R. R. DANIEL, S. HOREN, J. L. LACY and J. E. ZIPSE: *Astron. Astrophys.*, **188**, 145 (1987).
[15] D. MULLER and K. K. TANG: *Astrophys. J.*, **312**, 183 (1987).
[16] J. KOTA: *Proceedings of the XIX International Cosmic Ray Conference*, Vol. **9** (La Jolla, 1985), p. 275.
[17] K. NAGASHIMA, R. TATSUOKA and S. MATSUZAKI: *Nuovo Cimento C*, **6**, 550 (1983).
[18] G. STEIGMAN: *Annu. Rev. Astron. Astrophys.*, **14**, 399 (1976).
[19] S. WEINBERG: *Phys. Rev. Lett.*, **42**, 850 (1979).
[20] A. H. GUTH: *Phys. Rev. D*, **23**, 347 (1981).
[21] S. WEINBERG: *Phys. Rev. Lett.*, **50**, 387 (1983).
[22] S. W. HAWKING: *Mon. Not. R. Astron. Soc.*, **152**, 75 (1971).
[23] T. K. GAISSER, F. W. STECKER, A. K. HARDING and J. J. BARNARD: *Astrophys. J.*, **309**, 647 (1986).
[24] E. N. PARKER: *Space Sci. Rev.*, **9**, 651 (1969).
[25] W. I. AXFORD: *Proceedings of the XVII international Cosmic Ray Conference*, Vol. **12** (Paris, 1981), p. 155.
[26] L. H. SMITH, A. BUFFINGTON, G. F. SMOOT, L. W. ALVAREZ and M. A. WAHLIG: *Astrophys. J.*, **180**, 987 (1973).
[27] M. J. RYAN, J. F. ORMES and V. K. BALASUBRAHMANYAN: *Phys. Rev. Lett.*, **28**, 985 (1972).
[28] E. JULIUSSON, P. MEYER and D. MÜLLER: *Phys. Rev. Lett.*, **29**, 445 (1972).
[29] J. A. LEZNIAK and W. R. WEBBER: *Astrophys. J.*, **223**, 676 (1978).
[30] J. F. ORMES and P. S. FREIER: *Astrophys. J.*, **222**, 471 (1978).
[31] C. J. CESARSKY: *Annu. Rev. Astron. Astrophys.*, **18**, 289 (1980).
[32] M. GARCIA-MUNOZ, J. A. SIMPSON, T. G. GUZIK, J. P. WEFEL and S. H. MARGOLIS: *Astrophys. J. Suppl.*, **2**, 453 (1978).
[33] J. J. ENGELMANN, P. GOEET, E. JULIUSSON, L. KOCH-MIRAMOND, N. LUND, P. MASSE, I. L. RASMUSSEN and A. SOUTOUL: *Astron. Astrophys.*, **148**, 2 (1985).
[34] J. M. GRUNSFELD, J. L'HEUREUX, P. MEYER, D. MULLER and S. P. SWORDY: *Astrophys. J. Lett.*, **327**, L31 (1988).
[35] R. R. DANIEL and S. A. STEPHENS: *Space Sci. Rev.*, **10**, 599 (1970).
[36] K. C. ANAND, R. R. DANIEL and S. A. STEPHENS: *Astrophys. Space Sci.*, **36**, 169 (1975).
[37] E. A. BOGOMOLOV, G. I. VASILYEV, S. YU. KRUTKOV, N. D. LUBYANAYA, V. A. RAMANOV, S. V. STEPANOV and M. S. SHULAKOVA: *Proceedings of the 20th International Cosmic Ray Conference*, Vol. 2 (Moscow, 1987), p. 72.

[38] S. P. AHLEN, S. BARWICK, J. J. BEATTY, C. R. BOWER, G. GERBIER, R. M. HEINZ, D. LOWDER, S. MCKEE, S. MUFSON, J. A. MUSSER, P. B. PRICE, M. H. SALOMON, G. TARLE, A. TOMASCH and B. ZHOU: *Phys. Rev. Lett.*, **61**, 145 (1988).
[39] R. E. STREITMATTER, S. STOCHAJ, J. F. ORMES, R. L. GOLDEN, S. A. STEPHENS, T. BOWEN, A. MOATS and J. LOYD-EVANS: to appear in *Advances in Space Research* (Pergamon Press).
[40] R. L. GOLDEN, G. D. BADHWAR, J. L. LACY and J. E. ZIPSE: *Nucl. Instrum. Methods*, **148**, 179 (1978).
[41] J. J. BEATTY, S. P. AHLEN, A. D. TOMASCH, B. ZHOU, C. R. BOWER, R. M. HEINZ, S. L. MUFSON, J. REYNOLDSON, T. G. GUSIK, J. MICHELL, J. P. WEFE, D. CRARAY, S. MCKEE, J. MUSSER and G. TARLE: *Proceedings of the XX International Cosmic Ray Conference*, Vol. 2 (Moscow, 1987), p. 374.
[42] T. SUGITATE, Y. AKIBA, S. HAYASHI, Y. MIAKE, S. NAGAMIYA and M. TORIKOSHI: *Nucl. Instrum. Methods A*, **249**, 354 (1988).
[43] J. F. ORMES, V. K. BALASUBRAHMANYAN, J. LLOYD-EVANS, R. E. STREITMATTER, T. BOWEN and R. L. GOLDEN: unpublished report (1986).
[44] S. SUZUKI, T. SUZUKI, T. MATSUSHITA and H. KUME: *IEEE Trans. Nucl. Sci.*, **33**, 377 (1986).
[45] J. F. ORMES, M. ISRAEL, M. WIEDENBECK and R. MEWALDT: in *The Particle Astrophysics Magnet Facility, Astromag, 1988*, unpublished report.
[46] J. L. LACY and R. S. LINDSEY: *Nucl. Instrum. Methods*, **148**, 179 (1974).
[47] C. W. FABJAN, W. WILLS, I. GAVRIENKO, S. MAIBUROV, A. SHMELEVA, P. VASELJEV, V. CHERNYATIN, B. DOLGOSHEIN, V. KANTSEROV, P. NEVSKI and A. SUMAROKOV: *Nucl. Instrum. Methods*, **185**, 119 (1981).
[48] U. AMALDI: *Phys. Scr.*, **23**, 409 (1981).
[49] S. PENSOTTI, P. G. RANCOITA, A. SEIDMAN and L. VISMARA: *Nucl. Instrum. Methods A*, **265**, 261 (1988).
[50] G. M. GARIBIAN, L. A. GEVORGIAN and C. YANG: *Nucl. Instrum. Methods*, **125**, 133 (1975).

● RIASSUNTO

In questo articolo viene presentato l'esperimento WiZard che sarà effettuato sulla Stazione Spaziale americana Freedom. L'apparato funzionerà sulla facility Astromag come uno spettrometro magnetico dedicato alla ricerca di antimateria primordiale nella radiazione cosmica. Con tale apparato saranno pure indagate, e sono qui discusse, varie altre questioni nel campo dell'astrofisica e della cosmologia come i solar flares, l'anisotropia galattica, gli spettri di nuclei piú pesanti (dal carbonio al ferro), l'astronomia a raggi gamma e altro. Si descrive inoltre la configurazione dell'apparato, la sua integrazione e la composizione di ogni rivelatore e si illustrano pure le operazioni a terra e in volo nonché la riduzione e l'analisi dei dati. Infine, si delineano la pianificazione della missione e le operazioni a bordo dell'equipaggio.

Резюме не получено.